Exploration of ammonium sulfate as a by-product using loaded clinoptilolite from swine permeate at high pHs with sodium sulfate

by

Jaime Herrera

B.S., California Polytechnic State University, Pomona, 2022

A REPORT

submitted in partial fulfillment of the requirements for the degree

MASTER OF SCIENCE

Department of Civil Engineering
Carl R. Ice College of Engineering

KANSAS STATE UNIVERSITY
Manhattan, Kansas

2024

Approved by:
Major Professor
Dr. Prathap Parameswaran

Copyright

Abstract

Population is expected to increase both globally and domestically, increasing the demand for food, water, energy, and resources. To meet this food demand and to keep costs relatively low to the consumer, industrial farming methods have increased in the past decades in the form of concentrated animal feeding operations (CAFOs). These concentrated/confined animal feeding operations (CAFOs) are characterized by the amount, type of livestock and by having minimal to insufficient surrounding agricultural land where the manure from these operations can be applied. Conventional storage practices and overapplication pose an environmental threat as surface runoff, leaching, and/or devastating breach due to the excessive amount of solids, nutrients, biological oxygen demand (BOD), and bacteria that threaten surface water, groundwater, air quality, human health, and wildlife. An emergent technology that can take advantage of the concentrated amounts of manure while removing solids, BOD, recycle water, provide the potential to extract nutrients and generate energy in the form of biogas, is an anaerobic membrane bioreactor (AnMBR). This type of technology has been commercialized in the food industry but is relatively novel in the application of manure and municipal treatment. Ongoing research at Kansas State University focuses on the treatment of swine manure from CAFOs. The goal of the AnMBR research team is to collect data, monitor parameters through various stages of the process, overcome membrane fouling, observe system performance, maintain desirable conditions for biogas producing organisms, recover nutrients from permeate, and determine final quality effluent after further polishing from artificial wetlands. This study focused on the nutrient recovery aspect of the AnMBR process, specifically the recovery of ammonia and ammonium ion from the permeate using clinoptilolite (CLI) zeolite and the regeneration of the CLI to create a liquid fertilizer product in the form of ammonium

sulfate. Numerous studies have shown the kinetics and affinity of CLI towards cations. Varying studies have confirmed the affinity for cation exchange to generally follow a $Cs^{+}>Rb^{+}>K^{+}>NH_4^{+}>Ba^{2+}>Sr^{2+}>Na^{+}\approx Ca^{2+}>Fe^{3+}>Al^{3+}>Mg^{2+}\approx Li^{+}$ and $K^{+}>NH_4^{+}>Na^{+}>Ca^{2+}>Mg^{2}$ sequence, for competing cations in reagent solutions and sewage municipal wastewater, respectively. Previous studies have also shown successful regeneration of CLI above 69% with a brine solution. Lastly, a recent study discovered high efficiency regeneration of CLI, above 90%, using sodium sulfate solution and sodium hydroxide at a pH that ranged from 12.6-12.9 that created an ammonium sulfate product. Influenced by the knowledge of previous studies and behavior of CLI, the experiments conducted in this study sought to create a non-saline regenerant with an ammonium sulfate by-product; at a relatively lower pH with the use of sulfuric acid, the use of permeate with its varying cations composition to displace ammonia/ammonium ions, the use of 1M sodium sulfate solution as a stand-alone regenerant, and 1 M sodium sulfate with the combination of sodium hydroxide at pHs of 8, 9, 10 and 12. The experiments demonstrated that the use 1M sodium sulfate and minimal amounts of sodium hydroxide as a regenerant at pH 9 yielded the highest ammonia/ammonium desorption rate from clinoptilolite loaded with ammonia-N derived from swine AnMBR permeate. The other conditions revealed variable levels of ammonia-N release, but below the pH 9 condition described above. The methodology, results, and discussion of these experiments will be further explained in this report.

Table of Contents

List of Figures

List of Tables

Acknowledgements

I would like to thank God for providing me and my loved ones with good health, vitality, and unconditional love. This research was partly supported by NSF National Research Traineeship (NRT) award #1828571. I would like to extend my utmost gratitude to Dr. Prathap Parameswaran for providing me with an opportunity to enhance my educational journey, further my knowledge, extended enlightenment, and for his honest mentorship. Thank you for your patience and understanding throughout this dynamic period in my life. I am grateful for this challenge and for Cal Poly Pomona's Dr. Monica Palomo and Dr. Omar Mora for believing in my success and potential. I aim to not take life, or anyone for granted and hope that this experience has been truly fulfilled to the best of my abilities. I would also like to thank the K-State faculty, Dr. Hettiarachchi, Dr. Im, Dr. Derby, Mirit, Dr. Koehn, Professor Dodds, thanks for taking the time to talk to me on a personal level on more than one occasion beyond academics. I am sure that the future generation should be well taken care of with deeper connections that go along with excellent transfer of knowledge. I am also incredibly pleased to have shared pain, sweat, complains, and tears from the all the lab work, course work, and life with my cohort and colleagues. Thank you, Jordan and Skye, for being open to conversation since day one. Jordan, thanks for being a dependable friend that always listens and for being unapologetically you. Skye, thanks for reminding me what hard work, time management, and commitment are in a person. Much love and respect. Special thanks to Dr. Arvind Kannan who continued mentoring me after he completed his research and asked my many questions I had for him. I would like to thank the rest of my colleagues past and present Mason, Caitlin, Nick, Jack, Brooke, Marc, Maria, Chinmay, Dr. Tran, Jessica, Moises, Lucas and the rest of the NRT crew. I am grateful for the Manhattan community for having great and caring neighbors, for the Qdoba

crew providing me with fuel and friendship, the ATA bus drivers for carrying conversations with me, and to the K-State's CE office crew.

To my faithful support group, loved ones from back home, thanks for keeping tabs on me to the point where it was probably a distraction and never making me feel alone. To my furry, best-canine friend forever and ever, Bruce, thanks for putting up with my late study nights, unquestioned loyalty, companionship, and the long road trips. I wish you could understand how much you have grounded me and reminded me to live in the present. Gracias especialmente a ti madre, ¡lo logramos! And lastly, to everyone whom I have met that has helped shape me into the man that I am today in this awesome journey of mine, deepest thanks, I appreciate you all!

Introduction

The increasing population domestically and worldwide has led to the rise of industrial farming methods in the form of concentrated animal feeding operations (CAFOs). The additional amounts of livestock head while simultaneously experiencing a decline in the number of farms have exacerbated the amount of waste excreted and use of water resources in a small geographic footprint. The Anaerobic Membrane Bioreactor technology platform seeks to take advantage of the concentrated waste and convert swine manure into water for indirect reuse, biogas which can be used as an energy source, and provides the opportunity to recover macronutrients such as ammonia-nitrogen and phosphate in the form of bioavailable fertilizer products. The purpose of these experiments was to recover ammonia/ammonium ion after Anaerobic Membrane Bioreactor (AnMBR) filtration with a clinoptilolite (CLI) zeolite adsorption process and subsequently maximize the release of ammonia/ammonium ion using sodium sulfate as a regenerant at various pHs (8, 9, 10, 12). The objective is to create a liquid ammonium sulfate solution that can be used as an alternative to the traditional combination of soil and fertilizer for use in hydroponic production systems.

Chapter 1 - Background and Literature Review

1.1 Concentrated animal feeding operations (CAFOs)

According to the United Nations, the global population is expected to increase to 8.6 billion in 2030 and approximately 9.8 billion in 2050, from 7.6 billion as of 2022. (UN 2021) Domestically, the U.S. Census Bureau in 2017 projected that the U.S. population would increase from 332.6 million in 2020 to 355.1 million in 2030 and approximately 390 million in 2050. (Vespa 2020) To meet the rise in demand, the production of livestock and poultry in the United States has approximately doubled since the 1950s. Farming methods have shifted away from small farms to concentrated animal feeding operations (CAFOs) in livestock and poultry in the past decades since the late 1950s. CAFOs are characterized by the U.S. Environmental Protection Agency as an animal feeding facility that contains over 1000 animal units or as assigned by their respective state designation due to their waste production and potential for pollutant discharge. Moreover, animal units are characterized as 1000-pound animal/livestock and must be housed at these localities for a minimum of 45 days in a one-year period. (US EPA 2004) Furthermore, CAFOs are also known to have no agricultural crops for direct application since manure, when adequately applied, serves as fertilizer. As of 2007, the U.S. Department of Agriculture estimated 2.2 billion livestock and poultry that produced nearly 1.1 billion tons of manure. (US EPA 2013) Livestock is defined by the U.S. Department of Agriculture (USDA) as the following animal types, feedlot beef, dairy cows, market swine and poultry. Feedlot beef or fattened cattle are steers and heifers that are fed to slaughter. Dairy cows or milk cows are female cattle that are bred and calved for their high milk production. Market swine are non-breeding hogs that are raised for slaughter. Confined poultry include chicken, hens, and turkeys. (USDA

2016a, 1999a, 2004). Further information on the total amount of livestock head and manure produced along with spatial distribution from can be found in the Appendix.

CAFOs must meet the requirements for obtaining a National Pollution Discharge Elimination System (NPDES), enforced by the Environmental Protection Agency under the Clean Water Act that is required for the discharge into waters of the U.S. due to their environmental hazard potential. (US EPA 2009) Since animal population density is condensed in small localities this creates a large demand for water and other resources and raises the risk of contamination in a precipitation event, lagoon overflow, spills due to storage failures, and/or improper/excessive application of manure. (US EPA 2013) As a result, CAFOs are labeled as source point of contamination that can negatively impact surface water, ground water due to the excessive volume of solids, biochemical oxygen demand (BOD), pathogens, heavy metals, antibiotics, hormones, pesticides, nutrients, and carbon content when the manure is abundantly applied, or the aforementioned events transpire leading to runoff and infiltration. (Gullick 2007) These substances are detrimental to human health, wildlife, water bodies, and emit greenhouse gases. (US EPA 2013) This report will emphasize the nutrient aspect of contamination.

Nutrients are characterized as necessary elements that are needed for living organisms to grow, and execute structural, functional biochemical activities. (Elser 2012; Rout 2016) Nitrogen (N) and phosphorous (P) are known as macronutrients for single-celled to complex/multicellular organisms due to their role in generation and development. (Wong 2015; Varjani 2017; Rout 2016; Mishra 2020) Nitrogen serves as the building blocks for cell wall components, proteins, and nucleic acids. (Howarth 2014; Saravanan 2021; Varjani and Upasani 2021) Animal excrement is composed of inorganic forms of nitrogen such as ammonia, NH_3. Ammonia is readily volatized into its gaseous, air pollutant, unpleasant odor form that is diffused in the air

once excreted. Ammonia and ammonium, NH_4^+, are toxic to aquatic wildlife, cause fish kills, and lead to eutrophication. Hence, ammonia can readily be assimilated by plants as the ammonium ion, NH_4^+. In the presence of oxygen, ammonia is converted to nitrite, NO_2^-, and then nitrate, NO_3^-, through nitrification by aerobic bacteria. Nitrate, NO_3^-, is the most common form of agricultural contaminant in groundwater due to its mobility in its surrounding soil characteristics and overapplication of manure. (US EPA 2004) Furthermore, nitrate, NO_3^-, is the cause of "blue baby syndrome" or methemoglobinemia, which can be fatal to infants, and therefore has a maximum concentration level (MCL) of 10 mg/L as a strict drinking water standard. (Goldstein 1974) Phosphorous mineralizes to stable orthophosphates which forms PO_4^{3-} (orthophosphate/phosphate), HPO_4^{2-} (hydrogen phosphate), $H_2PO_4^-$ (dihydrogen phosphate), and H_3PO_4 (phosphoric acid) depending on the pH. (Wong 2015) In addition, these compounds and linear polyphosphates can be hydrolyzed and converted to reactive, bio-available phosphate that can then be integrated by plants and used by aquatic life. (Mustafa 2010) Concentrations of phosphorous above 1 mg/L and nitrogen compounds above 10 mg/L in water bodies induces eutrophication in the form of harmful algal blooms. (Hamdan 2010) Harmful algal blooms are known to produce toxins that are toxic to fish and can also produce illness in humans and other wildlife. As algal biomass begins to die-off, the decay and decomposition results in the lack of oxygen for aquatic life causing a severe decline in organism biodiversity. (Yuan 2006) Due to these adverse effects to the environment, public health, and wildlife, the US Environmental Protection Agency (US EPA) has set a discharge limit for these nutrients as; .5-1.0 mg/L for phosphate, nitrate has to be below 10 mg/L, ammonia must remain under 5 mg/L, and nitrite must not exceed .1 mg/L. (US EPA 2009) However, the opportunity exists for the recovery of these nutrients and repurpose them for beneficial use, while removing them from the

wastewater. These options have not been researched with the intent of system adoption and is the motivation for this report.

1.2 Anaerobic membrane bioreactor (AnMBR)

The Anaerobic Membrane Bioreactor (AnMBR) is an emergent technology that uses anaerobic biological treatment for organic carbon conversion into biogas that contains a mixture of methane and carbon dioxide along with physical solid removal through membrane filtration. The biogas that is generated can be used for electricity, heat, or a form of alternative fuel for transportation vehicles. Moreover, the AnMBR system provides an environment for microorganisms to thrive while simultaneously removing suspended materials and these microorganisms from the treated effluent, also known as permeate, via a permeate pump. Research conducted on this technology has reached pilot-scale configuration for further experimentation, development, troubleshooting, and potential commercialized implementation in regard to municipal wastewater and swine waste. An extensive study of a gas-sparged AnMBR approximately for 472 days at Kansas State University demonstrated the pilot's scale ability to comply with EPA's standard of 30 mg/L for BOD_5, COD of 60 mg/L, total suspended solids, pH, amongst other objectives. (Evans 2019) The BOD_5 removal achieved an average removal of 88 ± 6% and a COD average removal of 88 ± 7%. (Lim 2019) Additionally, a lab-scale AnMBR at Kansas State University has also achieved COD removal efficiency greater than 80% and BOD_5 removal greater than 95%. (Kannan 2023) Although there have been great advances in the AnMBR platform, there are still bottlenecks that continuous research will seek to overcome, such as full-scale demonstration, membrane fouling, methane recovery, biosolids quality, and energy neutrality. (Evans 2019)

1.3 Ammonia adsorption and recovery from swine wastewater permeate using naturally occurring clinoptilolite (CLI)

Kannan et al 2021, Cooney et al 1999 confirmed the order of affinity that the clinoptilolite zeolite to be $K^{+}>Ca^{2+}>Na^{+}>Mg^{2+}$ and $K^{+}>NH^{4+}>Na^{+}>Ca^{2+}>Mg^{2+}$ with actual swine permeate and sewage respectively. Dr. Kannan conducted column studies to determine the breakthrough point of Zeobest, CLI at 10% of the initial ammonia/ammonium reading, with synthetic swine permeate and actual swine permeate along with exhaustion at 90% of the initial ammonia/ammonium reading. Kannan then plotted results for the duplicate run for graphical analysis and calculated the adsorption capacity and the total ammonia capture capacity. The experimental results were then compared to the Thomas model to determine the theoretical maximum ammonia adsorption capacity and adsorption rate on the column. (Thomas 1944) Also, the experimental results were contrasted to the Yoon-Nelson model for the predicted time needed to achieve 50% adsorbate saturation in the column. Moreover, the experimental data were compiled and simultaneously plotted together for visual representation and to denote the minor differences attributed to the CLI adsorption behavior of synthetic and actual swine permeate in the column studies.

Dr. Kannan also sought to quantify and determine the efficacy of .5M sodium chloride solution as a regenerant and conducted cyclical studies to calculate the efficiency of desorption. Kannan articulated that at a concentration of 400 mg/L NH_4-N, the brine solution was able to attain a desorption rate of 8.3 mg/g for the first cycle and desorb the captured ammonia/ammonium at an efficiency rate over 69% after 4 successful cycles.

1.4 Recovery of Ammonium Sulfate Solution by Regeneration of Loaded Clinoptilolite (CLI)

Clinoptilolite (CLI) is a type of zeolite that is extensively studied for its ion exchanging capabilities. The CLI structure is composed of aluminosilicates with SiO_4 and AlO_4^- connected by shared oxygen atoms. (Jha 2016) The negative charge is caused by the substitution of SiO_4 by AlO_4^- creating a negative charge. This allows cations such as Na^+, K^+, Ca^{2+}, and Mg^{2+}. In wastewater industries and research, CLI is used for the adsorption of ammonium, and its regenerative properties. Wasielewski's research team deduced that CLI can uptake a single form of cation when a sodium-containing solution is used as a regenerant, also referred as homionic. This form of CLI is desirable since it has been demonstrated that homionic CLI can achieve higher uptake capacity, can take up ammonium faster, and can alter pore diameters. Guo et al, demonstrated that the regeneration efficiency of a NaCl solution was improved from less than 70% to 90-95% efficiency by the addition of NaOH (.032-1M). The maximum efficiency by Guo's research team occurred with .34M NaCl solution and .1M NaOH. Wasielewski's team sought to produce an ammonium sulfate solution through the use of sodium sulfate as a regenerant and with the addition of sodium hydroxide at a pH range of 12.6-.9, with the best results occurring at a loading rate of 13.5 mg/g and a mixture of .25 n(Na2SO4)/n(NH4+ adsorbed) and .9n (NaOH)/n(NH4+ads) for dry sorbent. The n in this context refers to molar concentration. (Wasielewski 2022)

Chapter 2 - Methodology

2.1 Adsorption continuous run

The anaerobic membrane bioreactor (AnMBR) is subject to continuous, extensive, and rigorous testing to determine its performance under strenuous conditions. An important benchmark for Dr. Parameswaran's AnMBR team consisted of monitoring the following parameters: removal of solids, biological oxygen demand (BOD), chemical oxygen demand (COD), biogas production, alkalinity, phosphate, and ammonia parameters with a continuous feeding of raw swine slurry for 100 hours. The permeate, which refers to the AnMBR filtered product, was collected in empty 5-gallon water containers until filled and repeated until the end of the 100-hour run. Since the AnMBR process primarily aims to remove solids, BOD, COD, and gas production, the removal of ammonia is minimal and makes it available in the permeate which is mostly free of organics or other co-occurring moieties except inorganic ions. The objective of this study was to determine the time interval that CLI achieved 99 percent saturation with ammonia by running four adsorption columns in series, at which point the last column would then be removed, rinsed with distilled water, and loaded again with raw CLI following the procedure stated below. 99 percent saturation is equivalent to 1% or .01 of the initial ammonia reading, which ensured a very low ammonia concentration in the final swine permeate after ammonia capture. The ammonia adsorption process was conducted through four customized glass columns created by the Kansas State's Chemistry Glass Department. Since the media is to fill 75% of the entire column after the use of rubber stoppers, the volume of the glass column was filled with water and then poured into a graduated cylinder for volume approximation. This yielded an estimated volume of 340 mL and multiplying this value by .75 output the value of 255.5mL. Therefore, every time the column was to be filled with CLI the graduated cylinder will

be filled to approximately 255 mL then subsequently weighed using CGoldenwall Precision Lab scale. The CLI media used for ammonia/ammonium adsorption was obtained from Zeobest, Northern Filter Media, Iowa, USA. The CLI media was sieved prior to use using standard sieve size no 30 for small particles segregation. Smaller particles are considered undesirable since it can create a turbid mixture and lessen the amount of CLI media that can be regenerated if the particle media is to remain suspended. Ammonia/ammonium concentrations were initially analyzed using a 1 to 10 dilution and HACH® TNT 832 high range ammonia kit and HACH DR3900 spectrophotometer in duplicate. Calibration of the Cole Parmer Masterflex L/S peristaltic pump was set for 20 minutes of contact time and the experiment setup design was up-flow. That is, flow entered the CLI media from the bottom of the column in series. The start time of the experiment was recorded, and ammonia measurements were conducted at 4 through 12-hour intervals depending on the reading. As the membrane in the reactor became more strained with time, the concentration of the initial ammonia in the container also increased resulting in shorter interval ammonia measurements. Lastly, it is important to note that this was the first time using customized glassware for the team and myself and two glassware columns were lost consequently at the end of the experiment.

2.2 Sulfuric acid with distilled water as a regenerant for ammonium sulfate production

The ammonia adsorption process was conducted similarly as the 100-hour experiment but, two customized glass columns created by the Kansas State's Chemistry Glass Department were used instead of four. After the adsorption was complete the first column, the column closest to the raw permeate was removed and bottom opened to remove three fourths of the saturated CLI and allowed to dry for 24 hours. Several dilutions of sulfuric acid, 1M, .1 M, .01 M H_2SO_4

were created from a 5M sulfuric acid solution and poured into their respective separate glass Erlenmeyer flasks. Double distilled water with an 18-ohm conductivity was then measured using a 1 L volumetric flask and poured into a 1-liter borosilicate glass bottle. The pH meter VWR B10P Symphony was then calibrated and used to read the pH as varying amounts of sulfuric acid were added to reach a pH of 3. Afterwards, a volumetric flask of 250 mL was obtained, and the pH 3 solution was poured and then transferred to a 250 mL Erlenmeyer flask. Subsequently, the same process was repeated for the remaining solution. The flasks were then placed in an orbital shaker. 1 gram was weighed using CGoldenwall Precision Lab scale of saturated CLI, and repeated. The orbital shaker was then set at 150 setting, the saturated CLI poured, and the shaker was started. An initial sample of 5 mL was obtained for ammonia/ammonium analysis using HACH TNT 830 low range ammonia vials after pH adjustments accordingly using differing molarities of sodium hydroxide (1M, .1 M, and .01 M) along with (1M and .01M) of hydrochloric acid to obtain the optimal value of 7. The reasoning for this was the pKa value of ammonia/ammonium at 9.2 and the pH range of values that the manufacturer HACH recommended were from 4-8. Therefore, the pH values were all adjusted within a .1 plus or minus from pH 7 to represent an accurate value and consistent value with other experiments. Thus, the pH was then adjusted to 7 within a .1 difference when samples at the 0^{th}, 24^{th} hour were collected. The protocol was repeated to obtain a pH 2 solution. The amount of sulfuric acid was recorded to determine molarities of the diluted sulfuric acid solution.

2.3 Permeate as a Regenerant

Permeate is defined as the effluent following the filtration process of the anaerobic membrane bioreactor (AnMBR). The confirmation of the cation presence in swine permeate including the ammonium ions paved the concept for permeate product to be used as a regenerant

due to the cationic composition of the permeate and the absence of organic carbon and suspended solids indicated a greater likelihood of reliable ammonia recovery through the CLI adsorption process. The permeate experiments consisted of two variations, both experiments would have ammonia removed, with one set being subsequently used as a regenerant thereafter and the alternating set would consist of the removal of phosphate and alkalinity prior to use as a regenerant. The ammonia adsorption process was conducted through two customized glass columns created by the Kansas State's Chemistry Glass Department. After the adsorption process was complete as denoted by the ammonia concentration in the effluent, the remaining permeate in the columns was emptied and a 2 L beaker filled with double-distilled water was then pumped into the columns for an hour. Subsequently, the columns were emptied of the water/CLI mixture. Then, the first glass column, the column closest to the raw permeate input was removed and the bottom opened to remove three fourths of the saturated CLI which was allowed to dry for 24 hours. The CLI was later placed in an empty beaker and would serve as the source for saturated CLI for regeneration experiments with sodium sulfate mixture at various pH values. For the ammonia-free permeate, 10 grams of saturated CLI were weighed using CGoldenwall Precision Lab scale and placed in 1 liter borosilicate glass bottle with a magnetic bar and placed in a mechanical stirrer correspondingly. One beaker was placed in Komet's Cimarec Power Direct Stirrer set at 150 setting for sample 1, and the latter was sited in a Fisher Scientific's Fisher Stirrer at setting 1, the lowest functioning setting. The ammonia-free permeate solution was measured in a 500 mL volumetric flask and then poured in the first flask. Initial reading consisted of the pH via a calibrated VWR B10P Symphony before and after contact using with the CLI, temperature and ammonia/ammonium reading under 2 minutes which was recorded as the 0^{th} hour measurement. The same was done for the second flask, and the same

parameters were measured after the 3rd, 6th and 24th hour. For the phosphate-and-ammonia free permeate experiments, similar protocol was conducted with the difference that 5 grams of saturated CLI were weighed using CGoldenwall Precision Lab scale for each flask and the volume of the phosphate-ammonia-free permeate was measured in a 250 mL volumetric flask, in duplicate. These samples were subject to pH adjustments, where the samples obtained were diluted in 1:5 ratios in a Falcon™ 15mL conical centrifuge tube and differing molarities of sodium hydroxide (1M, .1 M, and .01 M) along with (1M and .01M) of hydrochloric acid were used accordingly to obtain the optimal value of 7. Ammonia/ammonium analysis was conducted using TNT 832 high range vials and HACH DR3900 spectrophotometer.

2.4 Regeneration of loaded clinoptilolite using sodium sulfate to create ammonium sulfate by-product

Fisher Scientific's anhydrous sodium sulfate was weighed to 142.04 g using CGoldenwall Precision Lab scale to produce a 1M solution. After the desired mass was obtained, the sodium sulfate crystals were then poured into a 1 L volumetric flask and filled with double distilled water until the 1 L mark in the volumetric flask neck. A magnetic bar was added in the volumetric flask and placed in Komet's Cimarec Power Direct stirrer until all the sodium sulfate crystals were dissolved. The saturated CLI from the permeate regenerant experiments were then weighed using CGoldenwall Precision Lab scale to obtain 10 grams, then repeated and placed into two adequately labeled 1-liter borosilicate glass. Next, the borosilicate glass labeled sample 1 was placed in Komet's Cimarec Power Direct stirrer and set at 150. As in previous experiments, the second sample was placed in Fisher's Scientific Fisher Stirrer at 1 setting. A 500 mL volumetric flask was obtained and filled with the sodium sulfate at the indicated marker and then poured into sample 1. The initial pH after contact was recorded, a 5 mL sample in a 15

mL Falcon™ centrifuge conical tube was then obtained and sequentially adjusted to a pH of 7 using a calibrated pH meter VWR B10P Symphony. The initial ammonia/ammonium, 0^{th} hour, reading was then analyzed using TNT 830 ultra-low range ammonia vials. The 3^{rd}, 6^{th}, and 24^{th} hour intervals were obtained using TNT 832 high-range ammonia vials. In addition, the temperature was recorded during these intervals. Lastly, a 500 to 1 sample was prepared for a measurement of the amount of sulfate present using a 15 mL Falcon™ conical centrifuge tube and 50 mL Centrifuge tube at the 24^{th} hour using TNT 865 high-range sulfate vials.

The experiment was repeated using contrasting molarities of sodium hydroxide (1M, .1 M, and .01 M) as necessary to raise the pH value of the sodium sulfate solution to 8, another experimental setup for pH 9, 10, and 12.




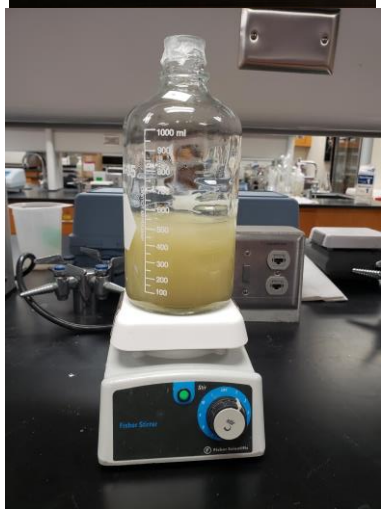

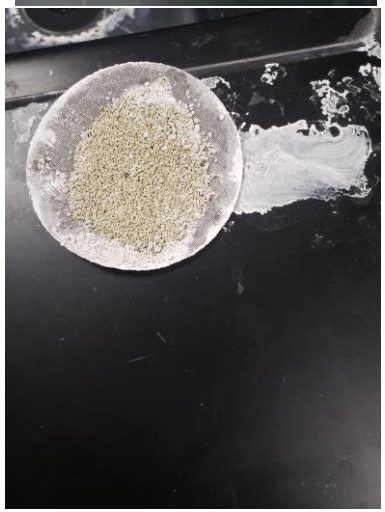

Figure 1. Experimental setup.

From top left and clockwise, saturation of CLI using a peristaltic pump and customized glass column, side by side comparison after 24-hour completion of ammonia-free permeate experiments, duplicate 1 in permeate experiments, white crystal precipitation after end of sodium sulfate at high pH experiments and air-dried, duplicate 2 during sodium sulfate as a regenerant experiment, and duplicate 1 during sodium sulfate as a regenerant experiment at high pH.

Chapter 3 - Results and Discussion

3.1 Adsorption continuous run

For the 100-hour continuous column run, the adsorption capacity at breakthrough was also calculated based on Kannan's adsorption equation. Where S (g/kg) is the adsorption capacity at time t (hour), M is the mass of the CLI in the column, Q (L/hr) is the flow rate pumping into the column multiplied by the run time (hr) which yields volume V (L). The ammonia concentration of the columns was calculated using the initial ammonia concentration, C_0, by the measured ammonia at the specified run hour. (Kannan 2021) (Cyrus 2011) The expected adsorption rates were low since breakthrough was targeted at nearly 1% of the initial ammonia input. Additionally, this graph demonstrates the adsorption rates with respect to the time run, the adsorption rate values ranged from .036 g/kg to 6.2 g/kg. Moreover, a plot that demonstrated the ratio of the effluent in contrast with the influent of ammonia nitrogen was also graphically plotted.

$$S = \frac{(C0-C)V}{M}$$

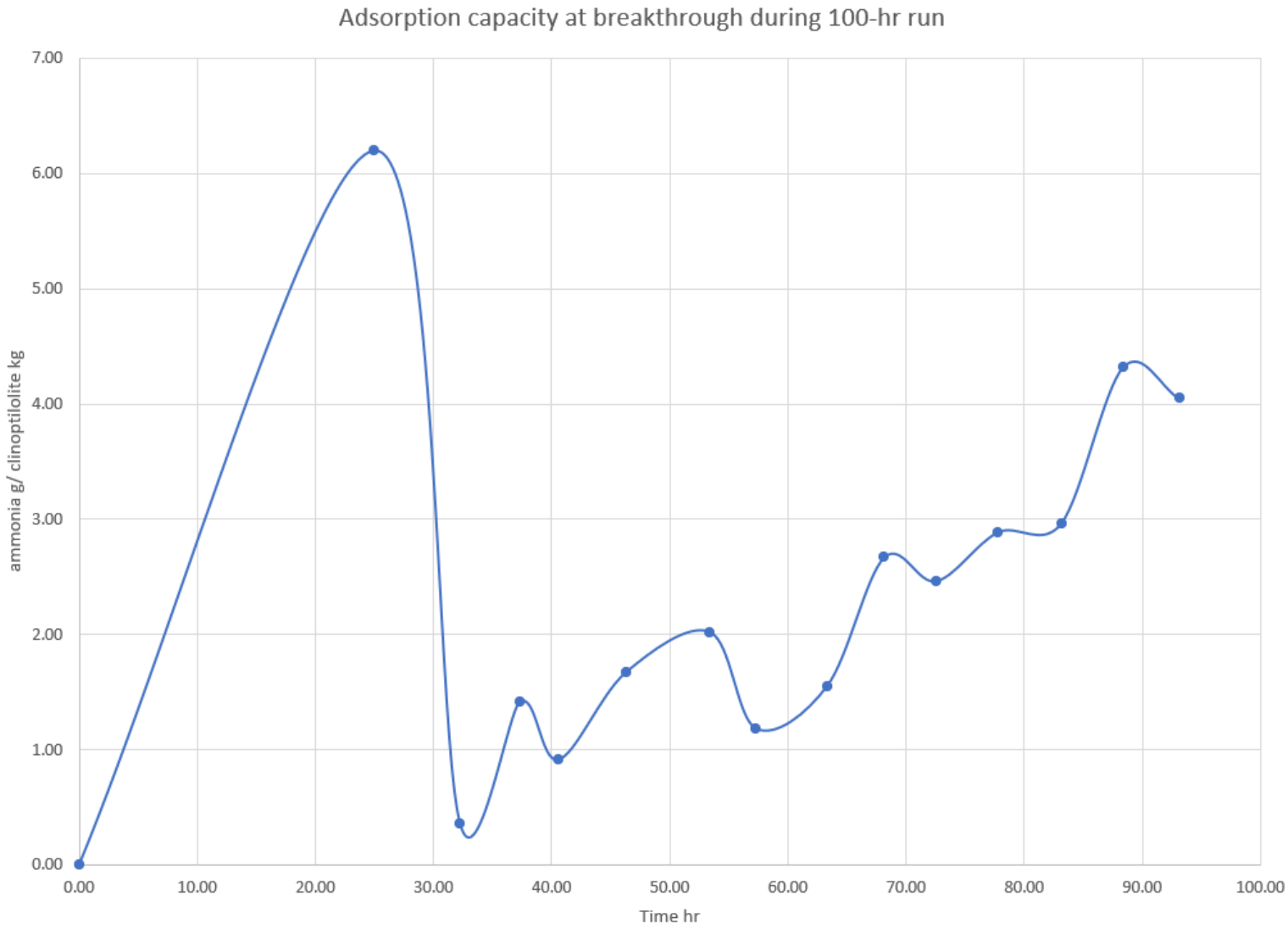

Figure 2 Graphical representation of breakthrough adsorption rate during 100-hr run with swine permeate obtained from a lab-scale AnMBR.

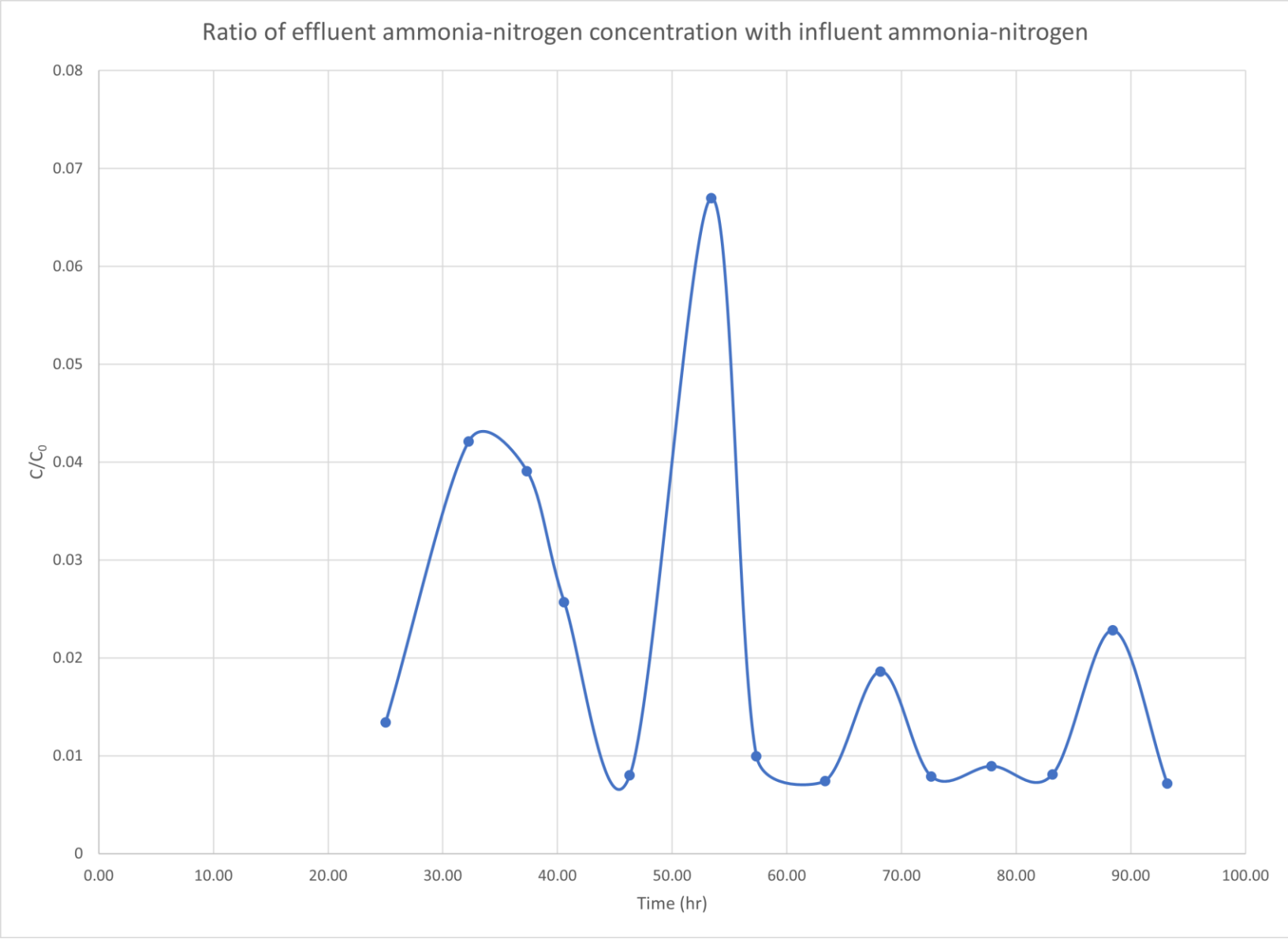

Figure 3 Breakthrough curve ratio of influent with effluent during 100-hr run with swine permeate obtained from a lab-scale AnMBR

The 100-hour graph demonstrated the adsorption capacity rate with respect to the run time in hours. In addition, the ratio of effluent ammonia-nitrogen with influent ammonia-nitrogen was graphically plotted. The adsorption capacity was low since the target breakthrough was at 1% of the initial ammonia nitrogen concentration. Also, the ratio of effluent with influent demonstrated that the target of 1% breakthrough was not met but the replacement of CLI media was consistently kept under 7% breakthrough. In contrast to Kannan's column studies in 2021, his initial ammonia/ammonium concentration and breakthrough point was considered at 10 % of the initial ammonia and through exhaustion to determine adsorption capacity. The continuous 100-hour conducted in October 2022 targeted the breakthrough to occur at 1% of the initial ammonia nitrogen missed the target due to team availability, lack of similar studies with respect to novel glassware, and the varying concentrations of ammonia as the membrane's performance declined under continuous strenuous conditions.

3.2 Sulfuric Acid with distilled water as a regenerant

The desorption rate was calculated using Kannan's formula for desorption.

$$q_d = \frac{C_d V}{M}$$

Where q_d in (mg/g) refers to the amount of ammonia that was desorbed, C_d refers to the concentration of ammonia released from the CLI in the regenerant solution (mg/L), V is the volume of regenerant used in Liters, and M is the mass of CLI. (Kannan 2021) The results from the initial experiments of saturated CLI with diluted sulfuric acid are tabulated. The desorption rate was calculated using Kannan's formula.

Table 1 Diluted sulfuric acid experiments with saturated CLI

pH~2 (hr)	pH	pH adj	Mass of CLI (g)	NH_3-N (mg/L)	Desorption rate (mg/g)
0	2.05 2.05	6.77 7.31	1.0112 1.0142	1.31 1.33	
24	2.4 2.41	7.57 6.95		17.4 20.6	1.721 2.031
pH~3 (hr)	**pH**	**pH adj**	**Mass of CLI (g)**	**NH_3-N (mg/L)**	**Desorption rate (mg/g)**
0	3.11 3.11	7.13 7.35	1.0121 1.0155	.595 .465	
24	6.99 7.01			11.3 8.3	1.116 .817

The diluted sulfuric acid experiments at pH 3, and 2 explored the potential of these mixtures to be used as a regenerant while simultaneously creating an ammonium sulfate product. The lower pH at 2 appeared to work as a better regenerant when compared to the desorption rate of pH 3. The diluted sulfuric acid experiments can be replicated with the same procedure as the sodium sulfate experiments, but initial experiments do not favor the use of diluted sulfuric acid as a regenerant although a low regenerant value was perceived. Lastly, since the saturated CLI used originated from the 100-hour continuous run, it is difficult to determine the desorption rate against the sorption rate since the sorption values are heterogenous and not homogeneous. As a result, the use of saturated CLI from the 100-hour batch were abandoned for the remaining experiments.

3.3 Permeate as a regenerant

Since the loaded CLI differed from the 100-hour adsorption studies, the sorption capacity was recalculated again using the same procedure. However, the initial ammonia concentration was 649 mg/L and final ammonia concentration was 0 mg/L. The volume that was ran through the CLI columns was approximately 2.01 L and the mass of the CLI was 493.29 g. This yielded a

sorption capacity of 2.64 mg/g. This loaded CLI value was also used for the sodium sulfate experiments.

$$S = \frac{\left(\frac{649mg}{L} - 0\right)(2.01L)}{493.29\,g} = 2.64\,\frac{mg}{g}$$

The desorption rate was calculated using Kannan's formula for desorption.

$$q_d = \frac{C_d V}{M}$$

Where q_d in (mg/g) refers to the amount of ammonia that was desorbed, C_d refers to the concentration of ammonia released from the CLI in the regenerant solution (mg/L), V is the volume of regenerant used in Liters, and M is the mass of CLI. (Kannan 2021)

Table 2 Data collected for permeate as a regenerant experiments

2:1 ratio P-NH_3-free-permeate (hr)	**pH**	**pH adj**	**NH_3-N 1:20 (mg/L)**	**NH_3-N (mg/L)**	**Desorption rate (mg/g)**
0	8.12 8.13	6.93 6.89		N/A 3.13	N/A .156
3	7.95 7.93	6.99 6.96	6.45 7.34	32.25 36.7	1.606 1.8424
6	7.96 7.95	7.01 6.95	8.12 7.06	40.6 35.3	2.022 1.754
24	7.97 8.05	6.96 6.90	8.14 7.24	40.7 36.2	2.027 1.799
NH_3-free permeate (hr)	**pH**	**pH adj**	**NH_3-N 1:20 (mg/L)**	**NH_3-N (mg/L)**	**Desorption rate (mg/g)**
0	8.33 8.33	6.98 7.01	.735 1.39	.735 1.39	.037 .069
3	7.95 7.93	6.99 6.96	6.45 7.34	32.25 36.7	1.616 1.871
6	7.96 7.95	7.01 6.95	8.12 7.06	40.6 35.3	1.301 1.868
24	7.97	6.96	8.14	40.7	1.643

	8.05	6.90	7.24	36.2	1.728

Extensive use and research on CLI media has documented the affinity that CLI has for cations. The results of this study demonstrated that ammonia-phosphate-free permeate functioned as the better regenerant when compared to ammonia-free permeate. It is important to note that the ammonia-phosphate-free permeate was conducted at half the scale of the ammonia-free permeate and would be strongly recommended to repeat the experiment at the same scale. The reason for the smaller scale experiment was due to the output that this experiment has during the phosphate capture process. Approximately 1 liter is used for the phosphate capture experiment and towards the end of the process approximately three fourths is the yield. Additionally, further loss of the final product is experienced when the ammonia-phosphate-free permeate was run through the CLI column since one-third of the input permeate remained inside the column. Furthermore, the ammonia-phosphate-free permeate was stripped from its alkalinity and this could prove noteworthy. As previously mentioned, the experiment should be repeated at the same scale which signifies that a larger volume should be used in the phosphate recovery experiments or the ammonia-free permeate round of experiments can be halved for direct comparison.

3.4 Sodium sulfate as a regenerant to create ammonium sulfate by-product at varying high pHs experiments

The results from the addition of sodium hydroxide and sodium sulfate are graphed in the following figures. In addition, the numerical data has been tabulated and is provided in Table 3, 4 and Table 2. Also, the graphs that are with respect also have the average pKa value as a vertical line from their respective sample. The highest observed desorption rate occurred at 1M sodium sulfate with the addition of sodium hydroxide that raised the initial pH of the solution to

9 at 6.35 mg/g and 6.2 mg/g in duplicate. Unless otherwise stated, the descending order at the 24th hour after pH ~ 9 was 1M sodium sulfate at 5.719 mg/g and 5.295 mg/g, pH~12 mixture at 5.539 mg/g and at the 6th hour 4.965 mg/g, pH~8 mixture at 4.741 mg/g and 4.416 mg/g, pH~10 mixture at 4.371 mg/g and 4.45 mg/g, and last was 2 to 1 ammonia-phosphate-free permeate at 2.027 mg/g and 1.799 mg/g. As previously mentioned, the desorption rate was calculated using Kannan's formula for desorption.

$$q_d = \frac{C_d V}{M}$$

Where q_d in (mg/g) refers to the amount of ammonia that was desorbed, C_d refers to the concentration of ammonia released from the CLI in the regenerant solution (mg/L), V is the volume of regenerant used in Liters, and M is the mass of CLI. (Kannan 2021)

Next, the amount of ammonium ion and the ammonia compound in their respective solution mixture was calculated in mg/L. The amount of NH3-N in mg/L that is measured by the HACH TNT vials, and the DR 3900 spectrophotometer is the total ammonia-nitrogen in the solution. However, if the temperature and pH of the solution is also measured in sampling then the equilibrium constant for that solution can be calculated. The equilibrium constant is then used to determine the unionized fraction of ammonia-nitrogen in the solution. The difference between the total ammonia-nitrogen and the unionized ammonia-nitrogen equates to the ammonium-ion nitrogen in the solution. Finally, the molecular weight of either species can be multiplied over 14 to output the value of the desired ammonia, ammonium ion concentration in mg/L. Emerson et al., determined the following equation to calculate the equilibrium constant, pka, where T is temperature.

$$pKa = \frac{.09108+2729.92}{(273.2+T)}$$

Next, Clement and Merlin 1995 determined the percentage of unionized ammonia.

$$unionized\ NH_3\ (\%) = \frac{100}{(1+10^{(pKa-pH)})}$$

$$Total\ NH_3 - N\ \left(\frac{mg}{L}\right) = NH_3 - N\left(\frac{mg}{L}\right) + NH_4^+ - N\left(\frac{mg}{L}\right)$$

$$NH_3 - N\ \left(\frac{mg}{L}\right) x\ unionized\ NH_3(\%\ in\ decimal)\ = NH_3\ (\frac{mg}{L})$$

$$NH_3 - N\ \left(\frac{mg}{L}\right)\ x\ \frac{17}{14} = NH_3(\frac{mg}{L}) \quad \text{or} \quad NH_4 - N\left(\frac{mg}{L}\right) x\left(\frac{18}{14}\right) = NH_4^+(\frac{mg}{L})$$

$$Hcc = \frac{cG}{cL}$$

The desorption experiments routinely occurred at a pH value higher than the pKa value of 9.26-28 where ammonia and the ammonium ion are determined to be in equilibrium. It is also scientifically known that ammonia volatilizes into its gas phase at equilibrium during this pH. Therefore, an estimated concentration of gaseous ammonia was calculated using the dimensionless Henry's constant. Two methods that were used to determine the concentration of ammonia gas in mg/L involved the calculated experimental value concentration of ammonia in the liquid multiplied against the dimensionless Henry's constant. The second method involved the use of Visual Minteq 4.0. This software is used to determine speciation, concentration, and behavior of ions, cations given known parameters amongst other uses. In the Visual Minteq 4.0 home menu, the activity correction method was selected from Davis to SIT due to the high ionic strength of the used solution. The sodium cation, Na^+, was selected and added to the list as 2 molal and the sulfate anion SO_4^{2-}, was also added to the list as 1 molal. This requires the concentration unit on the top right in the home menu to be selected to molal for the previous ions. Next, the initial ammonium concentration of 649 mg/L was added to the list. Again, ensure that the correct concentration units are selected. After, the Multi-problem/Sweep option is selected to determine the concentration of the ions involved at varying pHs. Sweep: one

parameter is varied is checked and the sweep component is selected as pH. The lowest pH value for these experiments was 6.6 and was inputted, increment values of .1 and 55 was inputted for the number of problems. Save and back is clicked, which takes the user to the home menu and the Run button is selected. The problem no. with the down arrow changes the pH sweep variation by the given selections. The experimental pH values were copied and sorted to determine the values that would be required for analysis for the ammonia concentration. For every adequate pH, the print to Excel button was clicked and copied into a master spreadsheet. The concentration of ammonia was then multiplied times the dimensionless Henry's constant for ammonia the molecular weight of ammonia and the conversion factor of 1000 mL per L for all relevant pH values. The gaseous ammonia concentration value was then added to the calculated experimental value of ammonia and desorption rate was recalculated.

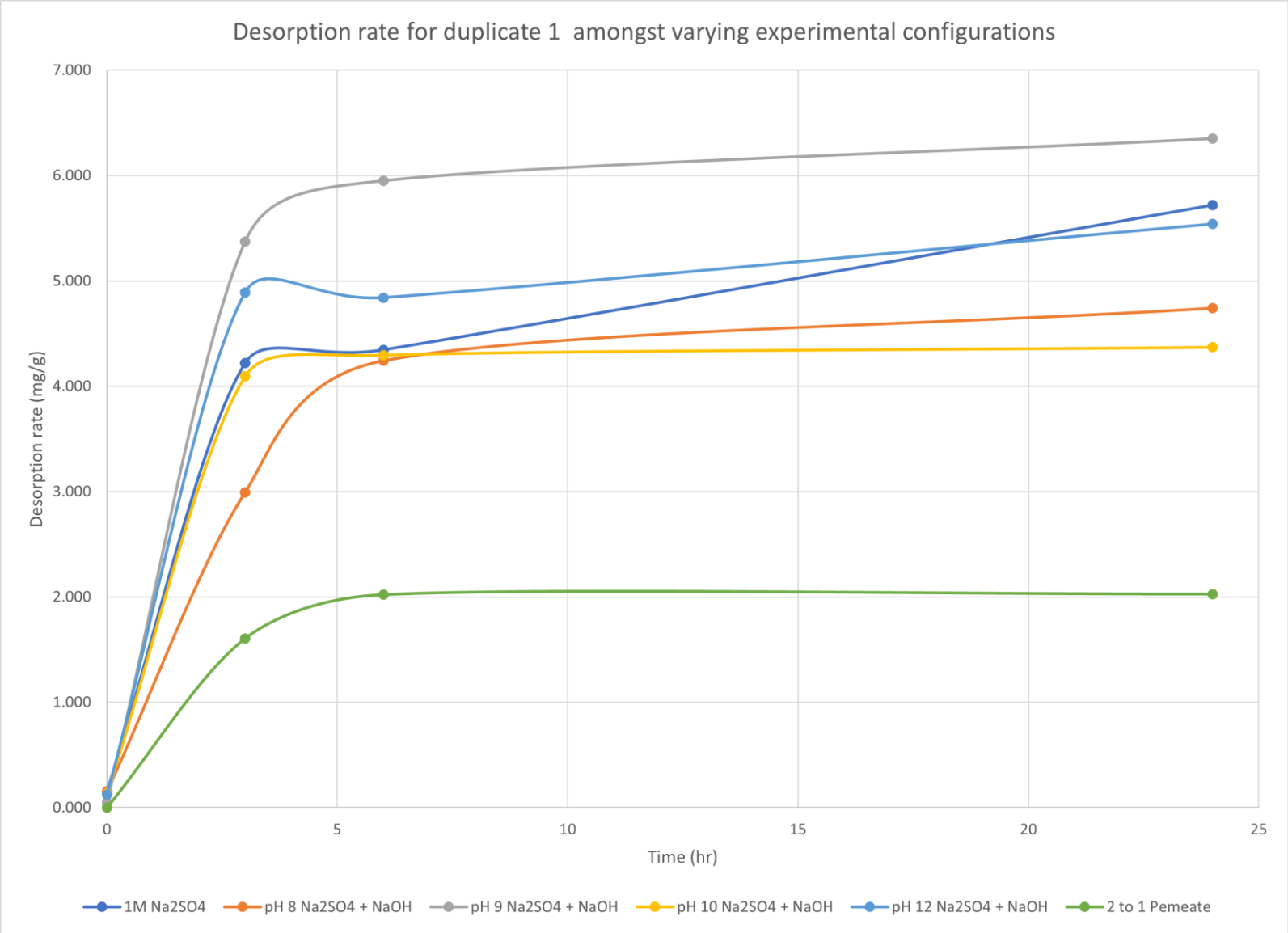

Figure 4. Desorption rate for duplicate 1 during length of experiment

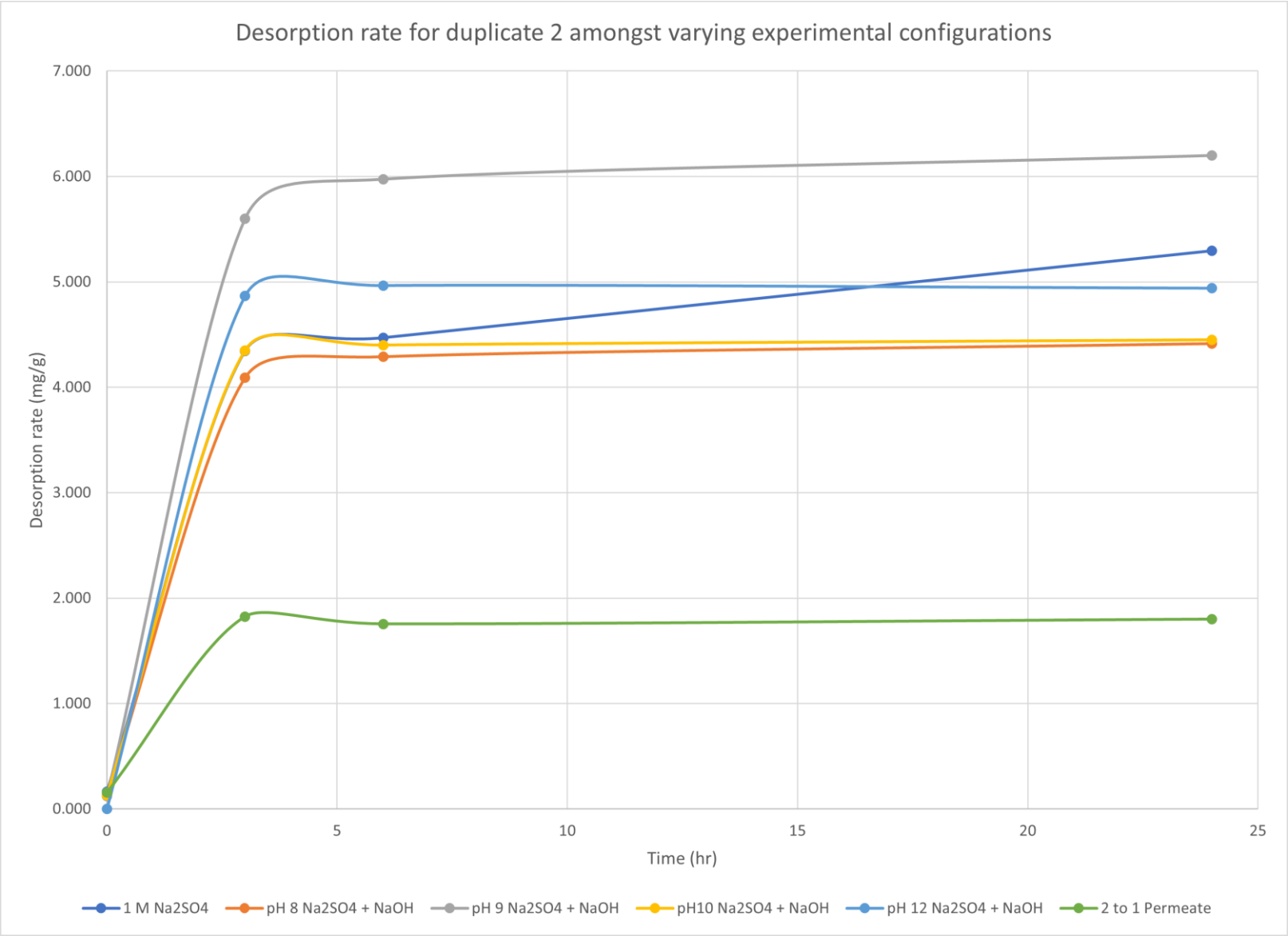

Figure 5. Desorption rate for duplicate 2 during length of experiment

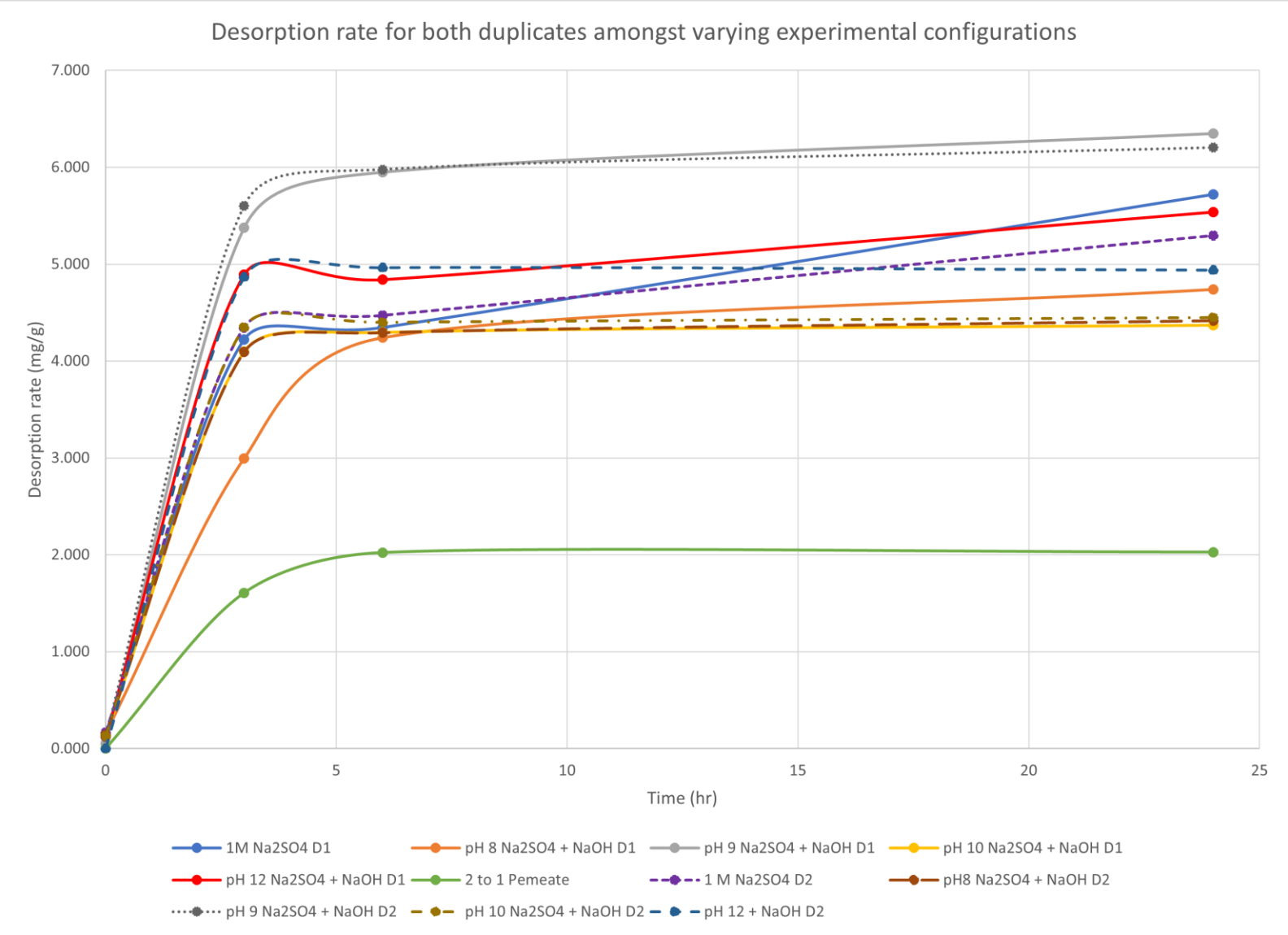

Figure 6. Comparison between both duplicates demonstrating the differing desorption rates after experimentation. Duplicate 2 results are denoted by dashed marks lines in the plot.

Table 3. Data collected and for sodium sulfate as a regenerant and ammonium sulfate by-product experiments

1 M Na2SO4 (hr)	**T (℃)**	**pH**	**pKa**	**% un-ionized NH3**	**Actual NH3 (mg/L)**	**Remaining NH4+ %**	**Actual NH4+ (mg/L)**
0	23	6.6	9.217	0.241	0.009	99.759	3.963
	23	6.6	9.217	0.241	0.010	99.759	4.245
3	25.5	8.94	9.140	38.706	39.715	61.294	66.592
	22.5	8.95	9.232	34.295	36.230	65.705	73.496
6	25	8.87	9.155	34.160	36.088	65.840	73.646
	24	8.98	9.186	38.372	41.702	61.628	70.917
24	26	9.15	9.124	51.475	71.569	48.525	71.436
	23	9.35	9.217	57.609	74.151	42.391	57.773
pH 8 ~ 1 M Na2SO4 + NaOH (hr)	**T (℃)**	**pH**	**pKa**	**% un-ionized NH3**	**Actual NH3 (mg/L)**	**Remaining NH4+ %**	**Actual NH4+ (mg/L)**
0	22.5	8	9.232	5.532	0.207	94.468	3.741
	22.5	8.01	9.232	5.654	0.194	94.346	3.421
3	25	8.21	9.155	10.194	7.427	89.806	69.279
	22.5	8.67	9.232	21.502	21.410	48.498	82.759
6	24.2	8.72	9.180	25.764	26.592	74.236	81.129
	22.5	9.01	9.232	37.472	39.131	62.528	69.138
24	25	9.16	9.155	50.290	58.013	49.710	60.718
	22	8.97	9.248	34.522	37.099	65.478	74.505
pH 9 ~ 1 M Na2SO4 + NaOH (hr)	**T (℃)**	**pH**	**pKa**	**% un-ionized NH3**	**Actual NH3 (mg/L)**	**Remaining NH4+ %**	**Actual NH4+ (mg/L)**
0	22	8	9.232	17.020	0.209	82.980	1.078
	21	8.01	9.232	12.391	0.366	87.609	2.737
3	25	8.21	9.155	19.529	25.492	80.471	111.223
	24.25	8.67	9.232	24.531	33.362	75.469	108.675
6	25.5	8.72	9.180	24.040	34.738	75.960	116.218
	24.25	9.01	9.232	34.519	50.090	65.481	100.606
24	25	8.84	9.155	32.624	50.311	67.376	110.015
	24	9.1	9.186	45.079	67.876	54.921	87.560

pH 10 ~ 1 M Na2SO4 + NaOH (hr)	**T (C)**	**pH**	**pKa**	**% un-ionized NH_3**	**Actual NH3 (mg/L)**	**Remaining NH4+ %**	**Actual NH4+ (mg/L)**
0	22.5	9.99	9.232	85.126	2.812	14.874	.520
	22.5	10	9.232	85.415	2.634	14.585	.476
3	26	9.11	9.124	49.173	48.962	50.827	53.586
	24.5	8.84	9.170	31.851	33.648	68.149	76.230
6	26	9.09	9.124	48.023	50.149	51.977	57.472
	25	8.82	9.155	31.620	33.788	68.380	77.367
24	26.5	9.14	9.109	51.775	55.011	48.225	54.253
	25.5	9.12	9.140	48.870	52.814	51.130	58.508
pH 12 ~ 1 M Na2SO4 + NaOH (hr)	**T (C)**	**pH**	**pKa**	**% un-ionized NH_3**	**Actual NH3 (mg/L)**	**Remaining NH4+ %**	**Actual NH4+ (mg/L)**
0	23.5	12	9.201	99.841	2.995	.159	.005
	23.5	12	9.201	99.841	N/A	.159	N/A
3	26.5	11.82	9.109	99.806	118.769	.194	.245
	25	11.83	9.155	99.789	118.143	.211	.264
6	26	11.78	9.124	99.779	117.526	.221	.275
	24.5	11.78	9.170	99.755	120.525	.245	.314
24	26.5	11.66	9.109	99.720	134.408	.280	.400
	25.5	11.69	9.140	99.719	119.877	.281	.357

Table 4. Additional data collected and calculated for sodium sulfate as a regenerant and ammonium sulfate as by-product experiments

1 M Na2SO4 (hr)	**pH**	**pH adj**	**NH_3-N 1:5 (mg/L)**	**NH_3-N (mg/L)**	**Desorption rate (mg/g)**	**SO_4^{2-} (mg/L)**
0	6.6 6.6	7.12 7.1		3.09 3.31	.154 .165	
3	8.94 8.95	6.95 6.91	9.109 9.155	84.5 87.0	4.221 4.346	
6	8.87 8.98	6.99 6.95	9.124 9.170	87.0 89.5	4.346 4.471	
24	9.15 9.35	7.09 7.05	9.109 9.140	114.5 106	5.719 5.295	92000 100000
pH 8 ~ 1 M Na2SO4 + NaOH (hr)	**pH**	**pH adj**	**NH_3-N 1:5 (mg/L)**	**NH_3-N (mg/L)**	**Desorption rate (mg/g)**	**SO_4^{2-} (mg/L)**
0	8 8.01	7.01 6.91		3.08 2.82	.154 .141	
3	8.21 8.67	6.91 6.92	12.0 16.4	60.0 82.0	2.994 4.092	
6	8.72 9.01	6.99 6.99	17.0 17.2	85.0 86.0	4.242 4.291	
24	9.16 8.97	7.15 6.95	19.0 17.7	95.0 88.5	4.741 4.416	99000 95000
pH 9 ~ 1 M Na2SO4 + NaOH (hr)	**pH**	**pH adj**	**NH_3-N 1:5 (mg/L)**	**NH_3-N (mg/L)**	**Desorption rate (mg/g)**	**SO_4^{2-} (mg/L)**
0	8.56 8.43	7.15 6.90		1.01 2.43	.0505 .1215	
3	8.54 8.69	6.99 6.99	21.5 22.4	107.5 112.0	5.375 5.60	
6	8.64 8.90	7.07 6.97	23.8 23.9	119.0 119.5	5.95 5.975	
24	8.84 9.10	7.13 6.89	25.4 24.8	127.0 124.0	6.35 6.20	118000 111000

pH 10 ~ 1 M Na2SO4 + NaOH (hr)	**pH**	**pH adj**	**NH_3-N 1:5 (mg/L)**	**NH_3-N (mg/L)**	**Desorption rate (mg/g)**	**SO_4^{2-} (mg/L)**
0	9.99 10.0	6.99 6.98		2.72 2.54	.136 .127	
3	9.11 8.84	6.98 7.2	16.4 17.4	82.0 87.0	4.096 4.35	
6	9.09 8.82	6.96 7.11	17.2 17.6	86.0 88.0	4.296 4.40	
24	9.14 9.12	6.94 6.90	17.5 17.8	87.5 89.0	4.371 4.45	114500
pH 12 ~ 1 M Na2SO4 + NaOH (hr)	**pH**	**pH adj**	**NH_3-N 1:5 (mg/L)**	**NH_3-N (mg/L)**	**Desorption rate (mg/g)**	**SO_4^{2-} (mg/L)**
0	12.0 12.0	7.02 7.04		2.47 N/A	.123 N/A	
3	11.82 11.83	7.09 6.9	19.6 19.5	98.0 97.5	4.890 4.865	
6	11.78 11.78	7.0 7.04	19.4 19.9	97.0 99.5	4.840 4.965	
24	11.66 11.69	7.11 6.91	22.2 19.8	111.0 99.0	5.539 4.940	103500 100100

Table 5. Data demonstrating estimated volatilization using dimensionless Henry's constant with calculated data and data from Visual Minteq

1 M Na2SO4 (hr)	pH	Actual NH3 (mg/L)	Total estimated NH3 (mg/L) w/ calculated volatilization	Total estimated NH3 (mg/L) w/ Minteq volatilization	Calculated desorption rate mg/g	Calculated desorption rate + calculated volatized	Calculated desorption rate + Minteq volatized
0	6.6	0.009	0.009	0.009	0.154	0.154	0.154
	6.6	0.010	0.010	0.010	.165	.165	.165
3	8.94	39.715	39.743	39.786	4.221	4.222	4.224
	8.95	36.230	36.256	36.301	4.346	4.347	4.349
6	8.87	36.088	36.113	36.135	4.346	4.347	4.348
	8.98	41.702	41.731	41.776	4.471	4.472	4.474
24	9.15	71.569	71.619	71.666	5.719	5.721	5.723
	9.35	74.151	74.203	74.293	5.295	5.297	5.301
pH 8 ~ 1 M Na2SO4 + NaOH (hr)	**pH**	**Actual NH3 (mg/L)**	**Total estimated NH3 (mg/L) w/ calculated volatilization**	**Total estimated NH3 (mg/L) w/ Minteq volatilization**	**Calculated desorption rate mg/g**	**Calculated desorption rate + calculated volatized**	**Calculated desorption rate + Minteq volatized**
0	8	0.207	0.207	0.216	0.154	0.154	0.154
	8.01	0.194	0.194	0.203	0.141	0.141	0.141
3	8.21	7.427	7.432	7.441	2.994	2.994	2.995
	8.67	21.410	21.425	21.451	4.092	4.092	4.093
6	8.72	26.592	26.611	26.638	4.242	4.242	4.243
	9.01	39.131	39.159	39.209	4.291	4.293	4.295
24	9.16	58.013	58.053	58.115	4.741	4.742	4.745
	8.97	37.099	37.124	37.176	4.416	4.417	4.419
pH 9 ~ 1 M Na2SO4 + NaOH (hr)	**pH**	**Actual NH3 (mg/L)**	**Total estimated NH3 (mg/L) w/ calculated volatilization**	**Total estimated NH3 (mg/L) w/ Minteq volatilization**	**Calculated desorption rate mg/g**	**Calculated desorption rate + calculated volatized**	**Calculated desorption rate + Minteq volatized**
0	8	0.209	0.209	0.240	0.0505	0.0505	0.0518
	8.01	0.366	0.366	0.391	0.122	0.122	0.123
3	8.21	25.492	25.510	25.523	5.375	5.376	5.376
	8.67	33.362	33.386	33.405	5.6	5.601	5.602
6	8.72	34.738	34.763	34.777	5.950	5.951	5.952

	9.01	50.090	50.125	50.154	5.975	5.976	5.978
24	8.84	50.311	50.346	50.369	6.350	6.351	6.352
	9.1	67.876	67.923	67.969	6.200	6.202	6.204
pH 10 ~ 1 M Na2SO4 + NaOH (hr)	**pH**	**Actual NH3 (mg/L)**	**Total estimated NH3 (mg/L) w/ calculated volatilization**	**Total estimated NH3 (mg/L) w/ Minteq volatilization**	**Calculated desorption rate mg/g**	**Calculated desorption rate + calculated volatized**	**Calculated desorption rate + Minteq volatized**
0	9.99	2.812	2.814	3.106	0.136	0.136	0.148
	10	2.634	2.636	2.929	0.127	0.127	0.139
3	9.11	48.962	48.996	49.055	4.096	4.097	4.100
	8.84	33.648	33.671	33.706	4.350	4.351	4.352
6	9.09	50.149	50.184	50.243	4.296	4.297	4.300
	8.82	33.788	33.812	33.844	4.400	4.401	4.402
24	9.14	55.011	55.05	55.113	4.371	4.372	4.375
	9.12	52.814	52.851	52.912	4.450	4.452	4.454
pH 12 ~ 1 M Na2SO4 + NaOH (hr)	**pH**	**Actual NH3 (mg/L)**	**Total estimated NH3 (mg/L) w/ calculated volatilization**	**Total estimated NH3 (mg/L) w/ Minteq volatilization**	**Calculated desorption rate mg/g**	**Calculated desorption rate + calculated volatized**	**Calculated desorption rate + Minteq volatized**
0	12	2.995	2.997	3.420	0.123	0.123	0.141
	12	N/A	N/A		N/A	N/A	N/A
3	11.82	118.769	118.852	119.194	4.890	4.894	4.908
	11.83	118.143	118.226	118.568	4.865	4.869	4.883
6	11.78	117.526	117.608	117.950	4.840	4.844	4.858
	11.78	120.525	120.610	120.950	4.965	4.969	4.983
24	11.66	134.408	134.502	134.831	5.539	5.543	5.556
	11.69	119.877	119.960	120.300	4.940	4.944	4.958

Undoubtedly, the desorption rate of ammonia/ammonium was highest with the use of sodium sulfate as a regenerant and with the addition of sodium hydroxide for a higher pH solution. The highest desorption rate occurred at the 24^{th} hour in experiments with a pH of 9 at 6.35 mg/g and 6.2 mg/g. These experiments were also considered successful as they created aqueous ammonium sulfate product. However, it is noteworthy to mention that ammonium/ammonia has a pKa value of 9.2, this is the value where the ammonium ion, NH_4^+ accepts an electron from the hydroxide ion, OH^- to become nonionic ammonia gas in equilibrium. Therefore, the values of ammonia/ammonium desorption rate could be skewed as time passes due to the volatilization of ammonia. An estimated amount of volatized ammonia was added to the amount of nonionized ammonia that was calculated and subsequently accounted for in desorption calculations. Typically, the Visual Minteq estimations accounted for higher concentrations of ammonia in gaseous form. These values are more apparent in the pH 12 experiments although the values only changed by approximately.018 mg/g in desorption. This coincides with the categorization of ammonia as a semivolatile compound by Henry's law constant. Furthermore, the highest value obtained in this experiment is less than the value obtained by Kannan during his batch experiment desorption studies with .5M NaCl at 8.3 mg/g at an adsorption value of 11.6 mg/g. Still, the desorption rate obtained by Kannan was at a lower initial concentration of 400 mg/L compared to the 649 mg/L that was used throughout this experiment. Nonetheless, the adsorption rate for this experiment was a low 2.69 mg/g, since the columns were not run through saturation and exhaustion, which should yield closer to the maximum possible adsorption rate. Hence it is recommended that future experiments have varying ranges of higher adsorption. Even so, the second desorption rate occurred with 1 M sodium sulfate at a pH of 6.6 and steadily increased its initial pH as the experiment continued to

9.15 and 9.35 at the end respectively. Lastly, the third highest desorption rate occurred at the initial high pH of 12.

Conclusion and Future work

In conclusion, it is highly recommended for verification of the collected data and to overcome some of the issues that were experienced due to novelty, the experiments should be repeated. A new mechanism was later used to avoid the breaking of delicate customized column glassware with success since the implementation of this procedure resulted in the avoidance of losing column glassware. Moreover, if the 100-hour adsorption studies are to be repeated, I would highly encourage that the future nutrient recovery team use three columns to begin as the data collected for these experiments occurred mostly with three active columns. The results of the adsorption studies for this experiment has resulted in the foundation for the expected behavior of CLI and an estimate of the intervals that ammonia readings should occur. Constant communication with the members of the nutrient recovery team is suggested so that the experiment remains continuous, and members can all have time to rest as needed. Lastly, pH adjustments of the sample are recommended for consistency and accuracy with all ammonia analysis.

The diluted sulfuric acid experiments should adapt the adsorption protocol from the permeate experiments followed by rinsing with double distilled water then drying for 24 hours to avoid false readings. As previously stated, the permeate experiments should be similar in volume for direct comparison. Furthermore, the alkalinity should be measured at the beginning of each set of experiments and at the end. Also, an experimental setup that removes the alkalinity of the ammonia-free permeate is strongly encouraged to determine if the alkalinity or the recovery of

bio-reactive phosphate is the cause of the better results when directly compared if this configuration of experiment is to be replicated.

Ammonium sulfate as a by-product and sodium sulfate as a regenerant experiments should be further analyzed for confirmation of the desired ions, ammonium/ammonia, NH_4^+, and sulfate, SO_4^{2-} by the soil analysis laboratory. Additional experiments of a higher pH at 12.6-12.9 along with an experiment at a lower pH, near 6 and another around 7 should also be conducted to compare results. As mentioned in the previous section, the next experimental setup should include varying higher adsorption rates such as 9, 11, and 13. Moreover, further experiments within the range of 9, such as 9.5 and 8.5 should be conducted to achieve a higher desorption rate, if possible. Since it was observed that the sulfate concentration was extremely high, a lower molarity solution of sodium sulfate is recommended to determine if results differ from the 1M solution that was used. Experiments should be conducted at millimolar strengths for contrast. Due to the lower desorption rates at higher pHs that was detected when compared to the pH of 9 experiments it is also strongly suggested that the experiments be closely monitored in shorter intervals after the 6^{th} hour and/or extended another 24 hours to determine if desorption increases under the starting pH conditions. The volatized ammonia concentration was calculated, and it was determined that volatilization occurs at a slow rate, however, it is best to conduct an experimental setup under the guidance of Dr. Hettiarachchi to attempt to quantify volatized ammonia gas during experimental run. Finally, all equipment used during experimentation should be calibrated as recommended by manufacturer specifications to ensure that values are accurate.

References

Clément, B., & Merlin, G. (1995). The contribution of ammonia and alkalinity to landfill leachate toxicity to duckweed. Science of the Total Environment, 170(1–2). https://doi.org/10.1016/0048-9697(95)04563-G

Cyrus, J. S., & Reddy, G. B. (2011). Sorption and desorption of ammonium by zeolite: Batch and column studies. *Journal of Environmental Science and Health, Part A*, *46*(4), 408–414. https://doi.org/10.1080/02773813.2010.542398

Damodara Kannan, A., Dillavou, J., H.H. Gamage, K., Randig, E., M. Hettiarachchi, G., & Parameswaran, P. (2023). Recovery of high-quality calcium phosphate fertilizer products from anaerobic membrane bioreactor treated swine wastewater. Chemical Engineering Journal, 453. https://doi.org/10.1016/j.cej.2022.139539

Damodara Kannan, A., & Parameswaran, P. (2021). Ammonia adsorption and recovery from swine wastewater permeate using naturally occurring clinoptilolite. Journal of Water Process Engineering, 43. https://doi.org/10.1016/j.jwpe.2021.102234

Emerson, K., Russo, R. C., Lund, R. E., & Thurston, R. v. (1975). Aqueous Ammonia Equilibrium Calculations: Effect of pH and Temperature. Journal of the Fisheries Research Board of Canada, 32(12). https://doi.org/10.1139/f75-274

Elser, J.J., 2012. Phosphorus: a limiting nutrient for humanity? Curr. Opin. Biotechnol. 23 (6), 833–838

Evans, P.; Doody, A.; Harclerode, M.; Vila, P.; Parameswaran, P.; Lim, K.; Bae, J.; Shin, C.; Lee, P.-H.; Tan, A.; et al. Anaerobic Membrane Bioreactor (AnMBR) for Sustainable Wastewater Treatment. Project ER-201434. Department of Defense Environmental Security Technology Program Final Report; Department of Defense: 2018, https://www.serdp-estcp.org/Program-Areas/Environmental-Restoration/Wastewater-and-Drinking-Water/ER-201434

Gullick, R.W., R.A. Brown, and D.A. Cornwell. 2007. Source water protection for concentrated animal feeding operations: a guide for drinking water utilities. Awwa Research Foundation and the U.S. Environmental Protection Agency. IWA Publishing.

Guo, X., Zeng, L., & Jin, X. (2013). Advanced regeneration and fixed-bed study of ammonium and potassium removal from anaerobic digested wastewater by natural zeolite. Journal of Environmental Sciences (China), 25(5). https://doi.org/10.1016/S1001-0742(12)60115-6

Hamdan, R., 2010. Aerated Blast Furnace Slag Filters for Enhanced Nitrogen and Phosphorus Removal from Small Wastewater Treatment Plants. The University of Leeds.

Howarth, R., 2014. Nitrogen in Freshwater Systems and Estuaries Nitrogen. *Reference Module In Earth Systems and Environmental Sciences*. Elsevier, NY, USA. https://doi. org/10.1016/B978-0-12-409548-9.09401-X.

Jha, B.; Singh, D.N. Basics of Zeolites. In *Fly Ash Zeolites*; Springer: Singapore, 2016; Volume 78; pp. 5–31

Körner, S., Das, S. K., Veenstra, S., & Vermaat, J. E. (2001). The effect of pH variation at the ammonium/ammonia equilibrium in wastewater and its toxicity to Lemna gibba. Aquatic Botany, 71(1). https://doi.org/10.1016/S0304-3770(01)00158-9

Lim, K., Anaerobic membrane bioreactors for domestic wastewater treatment: Treatment performance and fouling characterization. 2021, Kansas State University.

Lim, K., Evans, P. J., & Parameswaran, P. (2019). Long-term performance of a pilot-scale gas-sparged anaerobic membrane bioreactor under ambient temperatures for holistic wastewater treatment. Environmental Science and Technology, 53(13). https://doi.org/10.1021/acs.est.8b06198

McGuire, V.L., 2017, Water-level and recoverable water in storage changes, High Plains aquifer, predevelopment to 2015 and 2013–15: U.S. Geological Survey Scientific Investigations Report 2017–5040, 14 p., https://doi.org/10.3133/sir20175040.

Milbrandt, A., Seiple, T., Heimiller, D., Skaggs, R., & Coleman, A. (2018). Wet waste-to-energy resources in the United States. Resources, Conservation and Recycling, 137. https://doi.org/10.1016/j.resconrec.2018.05.023

Mishra, B., Varjani, S., Agarwal, D.C., Mandal, S.K., Ngo, H.H., Taherzadeh, M.J., Chang, J.S., You, S., Guo, W., 2020. Engineering biocatalytic material for the remediation of pollutants: a comprehensive review. Environ. Technol. Innov. 20, 101063.

Mustafa, A., 2010. Nutrient removal with integrated constructed wetlands: microbial ecology and treatment performance evaluation of full-scale integrated constructed wetlands.

Purwono, P., Hibbaan, M., Rezagama, A., & Budihardjo, M. A. (2017). Ammonia-nitrogen ($NH3^{-}N$) and ammonium-nitrogen ($NH4+^{-}N$) equilibrium on the process of removing nitrogen by using tubular plastic media. Journal of Materials and Environmental Sciences, 8(S).

Rout, P.R., Dash, R.R., Bhunia, P., 2016b. Development of an integrated system for the treatment of rural domestic wastewater: emphasis on nutrient removal. RSC Adv. 6 (54), 492.

Rout, P. R., Shahid, M. K., Dash, R. R., Bhunia, P., Liu, D., Varjani, S., Zhang, T. C., & Surampalli, R. Y. (2021). Nutrient removal from domestic wastewater: A comprehensive review on conventional and advanced technologies. Journal of Environmental Management, 296. https://doi.org/10.1016/j.jenvman.2021.113246

Saravanan, A., Kumar, P.S., Varjani, S., Jeevanantham, S., Yaashikaa, P.R., Thamarai, P., Abirami, B., George, C.S., 2021. A review on algal-bacterial symbiotic system for effective treatment of wastewater. Chemosphere 129540.

Tao, W., & Ukwuani, A. T. (2015). Coupling thermal stripping and acid absorption for ammonia recovery from dairy manure: Ammonia volatilization kinetics and effects of temperature, pH and dissolved solids content. Chemical Engineering Journal, 280. https://doi.org/10.1016/j.cej.2015.05.119

Thomas, H. C. (1944). Heterogeneous Ion Exchange in a Flowing System. Journal of the American Chemical Society, 66(10). https://doi.org/10.1021/ja01238a017

United Nations Department of Economic and Social Affairs Population Division. (2022). World Population Prospects 2022: Summary of Results. In United Nation (Issue 9).

US EPA. (2004). Risk assessment Evaluation for concentrated animal feeding operations. National Service Center for Environmental Publications (NSCEP).

US-EPA. (2013). Literature review of contaminants in livestock and poultry manure and implications for water quality. In Office of Water: Vol. EPA 820-R-.

Varjani, S.J., Gnansounou, E., Pandey, A., 2017. Comprehensive review on toxicity of persistent organic pollutants from petroleum refinery waste and their degradation by microorganisms. Chemosphere 188, 280–291.

Varjani, S., Upasani, V.N., 2021. Bioaugmentation of Pseudomonas aeruginosa NCIM 5514–A novel oily waste degrader for treatment of petroleum hydrocarbons. Bioresour. Technol. 319, 124240.

Vespa, J., Medina, L., & Armstrong, D. M. (2020). Demographic Turning Points for the United States: Population Projections for 2020 to 2060. In Current Population Reports.

Wasielewski, S., Rott, E., Minke, R., & Steinmetz, H. (2022). Recovery of Ammonium Sulfate Solution by Regeneration of Loaded Clinoptilolite. Nanomaterials, 12(3). https://doi.org/10.3390/nano12030525

Wong, A., 2015. Investigating the Enhancement of Biological Filtration with Capping Material Designs and Nutrient Amendments 36–49249.

Yuan, M., Carmichael, W. W., & Hilborn, E. D. (2006). Microcystin analysis in human sera and liver from human fatalities in Caruaru, Brazil 1996. Toxicon, 48(6). https://doi.org/10.1016/j.toxicon.2006.07.031 Booker, N. A., Cooney, E. L., & Priestley, A. J. (1996). Ammonia removal from sewage using natural australian zeolite. Water Science and Technology, 34(9), 17-24. Retrieved from https://er.lib.k-state.edu/login?url=https://www.proquest.com/scholarly-journals/ammonia-removal-sewage-using-natural-australian/docview/1943240684/se-2

Appendix A - Supplementary Information

Appendix Figure A.1. Livestock animal units as a total and per acre of farmland in 2007 by state

Rank Total AUs	State	AUs	Rank AUs/Acre Farmland	State	AUs/Acre Farmland
1	TEXAS	11,109,770	1	NORTH CAROLINA	0.32
2	IOWA	5,586,515	2	DELAWARE	0.26
3	NEBRASKA	5,235,899	3	PENNSYLVANIA	0.23
4	CALIFORNIA	5,235,439	4	VERMONT	0.22
5	KANSAS	4,932,902	5	WISCONSIN	0.21
6	OKLAHOMA	4,571,012	6	CALIFORNIA	0.21
7	MISSOURI	4,178,962	7	NEW YORK	0.20
8	MINNESOTA	3,268,570	8	VIRGINIA	0.19
9	WISCONSIN	3,213,092	9	IOWA	0.18
10	SOUTH DAKOTA	3,179,772	10	TENNESSEE	0.17
11	NORTH CAROLINA	2,704,347	11	FLORIDA	0.17
12	COLORADO	2,183,438	12	IDAHO	0.17
13	MONTANA	2,172,114	13	MARYLAND	0.16
14	ARKANSAS	2,164,456	14	ALABAMA	0.16
15	KENTUCKY	2,143,425	15	ARKANSAS	0.16
16	IDAHO	1,934,024	16	GEORGIA	0.16
17	TENNESSEE	1,901,829	17	KENTUCKY	0.15
18	PENNSYLVANIA	1,801,172	18	MISSOURI	0.14
19	ILLINOIS	1,623,316	19	OKLAHOMA	0.13
20	GEORGIA	1,582,445	20	MINNESOTA	0.12
21	FLORIDA	1,572,198	21	CONNECTICUT	0.12
22	VIRGINIA	1,540,785	22	SOUTH CAROLINA	0.12
23	NORTH DAKOTA	1,511,460	23	HAWAII	0.12
24	OHIO	1,486,479	24	NEBRASKA	0.12
25	ALABAMA	1,446,018	25	MICHIGAN	0.11
26	INDIANA	1,426,494	26	WEST VIRGINIA	0.11
27	NEW YORK	1,405,612	27	OHIO	0.11
28	NEW MEXICO	1,369,823	28	KANSAS	0.11
29	OREGON	1,182,494	29	LOUISIANA	0.10
30	MISSISSIPPI	1,171,555	30	MISSISSIPPI	0.10
31	MICHIGAN	1,136,740	31	INDIANA	0.10
32	WYOMING	1,101,102	32	MASSACHUSETTS	0.09
33	WASHINGTON	980,293	33	TEXAS	0.09
34	LOUISIANA	840,534	34	RHODE ISLAND	0.08
35	ARIZONA	813,626	35	NEW HAMPSHIRE	0.08
36	UTAH	760,972	36	SOUTH DAKOTA	0.07
37	SOUTH CAROLINA	586,368	37	OREGON	0.07
38	WEST VIRGINIA	394,816	38	COLORADO	0.07
39	NEVADA	380,843	39	UTAH	0.07
40	MARYLAND	333,955	40	WASHINGTON	0.07
41	VERMONT	268,767	41	NEVADA	0.06
42	DELAWARE	132,875	42	MAINE	0.06
43	HAWAII	130,823	43	ILLINOIS	0.06
44	MAINE	82,780	44	NEW JERSEY	0.06
45	CONNECTICUT	48,862	45	NORTH DAKOTA	0.04
46	MASSACHUSETTS	45,418	46	WYOMING	0.04
47	NEW JERSEY	41,652	47	MONTANA	0.04
48	NEW HAMPSHIRE	36,402	48	NEW MEXICO	0.03
49	ALASKA	11,903	49	ARIZONA	0.03
50	RHODE ISLAND	5,364	50	ALASKA	0.01
	U.S. TOTAL	**92,969,509**		**U.S. AVERAGE**	**0.12**

Credit: USDA 2009

Appendix Figure A.2. Total estimated livestock and poultry manure and estimated tons of manure per acre of farmland in 2007

Rank Total Manure	State	Tons Manure	Rank Tons Manure/Acre Farmland	State	Tons Manure/Acre Farmland
1	TEXAS	128,048,896	1	NORTH CAROLINA	3.85
2	CALIFORNIA	68,496,143	2	DELAWARE	3.81
3	IOWA	68,360,493	3	VERMONT	3.05
4	NEBRASKA	59,100,556	4	PENNSYLVANIA	2.99
5	KANSAS	55,792,510	5	WISCONSIN	2.80
6	OKLAHOMA	52,036,892	6	CALIFORNIA	2.70
7	MISSOURI	48,070,611	7	NEW YORK	2.66
8	WISCONSIN	42,531,594	8	MARYLAND	2.23
9	MINNESOTA	39,816,914	9	VIRGINIA	2.22
10	SOUTH DAKOTA	36,358,712	10	IOWA	2.22
11	NORTH CAROLINA	32,620,857	11	IDAHO	2.13
12	ARKANSAS	25,665,769	12	TENNESSEE	2.02
13	KENTUCKY	25,117,706	13	FLORIDA	2.01
14	COLORADO	25,022,958	14	GEORGIA	1.99
15	MONTANA	24,709,841	15	ALABAMA	1.98
16	IDAHO	24,532,956	16	ARKANSAS	1.85
17	PENNSYLVANIA	23,359,900	17	KENTUCKY	1.80
18	TENNESSEE	22,209,901	18	MISSOURI	1.66
19	GEORGIA	20,202,017	19	CONNECTICUT	1.62
20	ILLINOIS	19,190,293	20	OKLAHOMA	1.48
21	NEW YORK	19,084,031	21	MINNESOTA	1.48
22	FLORIDA	18,563,926	22	MICHIGAN	1.46
23	OHIO	18,460,395	23	SOUTH CAROLINA	1.41
24	VIRGINIA	18,029,169	24	HAWAII	1.33
25	ALABAMA	17,902,968	25	OHIO	1.32
26	INDIANA	17,368,868	26	NEBRASKA	1.30
27	NORTH DAKOTA	17,175,740	27	MISSISSIPPI	1.27
28	NEW MEXICO	17,173,686	28	WEST VIRGINIA	1.23
29	MICHIGAN	14,628,016	29	LOUISIANA	1.23
30	MISSISSIPPI	14,583,109	30	KANSAS	1.20
31	OREGON	13,989,238	31	INDIANA	1.18
32	WYOMING	12,472,771	32	MASSACHUSETTS	1.14
33	WASHINGTON	12,340,841	33	NEW HAMPSHIRE	1.03
34	ARIZONA	10,074,405	34	RHODE ISLAND	0.99
35	LOUISIANA	9,968,209	35	TEXAS	0.98
36	UTAH	8,938,890	36	OREGON	0.85
37	SOUTH CAROLINA	6,895,155	37	SOUTH DAKOTA	0.83
38	MARYLAND	4,578,248	38	WASHINGTON	0.82
39	WEST VIRGINIA	4,548,748	39	MAINE	0.82
40	NEVADA	4,459,013	40	UTAH	0.81
41	VERMONT	3,757,488	41	COLORADO	0.79
42	DELAWARE	1,944,044	42	NEVADA	0.76
43	HAWAII	1,490,546	43	ILLINOIS	0.72
44	MAINE	1,100,800	44	NEW JERSEY	0.71
45	CONNECTICUT	658,068	45	NORTH DAKOTA	0.43
46	MASSACHUSETTS	588,513	46	WYOMING	0.41
47	NEW JERSEY	521,513	47	MONTANA	0.40
48	NEW HAMPSHIRE	486,181	48	NEW MEXICO	0.40
49	ALASKA	137,131	49	ARIZONA	0.39
50	RHODE ISLAND	67,158	50	ALASKA	0.16
	U.S. TOTAL	**1,113,232,385**		**U.S. AVERAGE**	**1.50**

Credit: USDA 2009

Appendix Figure A.3. Manure production in continuous United States from data in high priority states

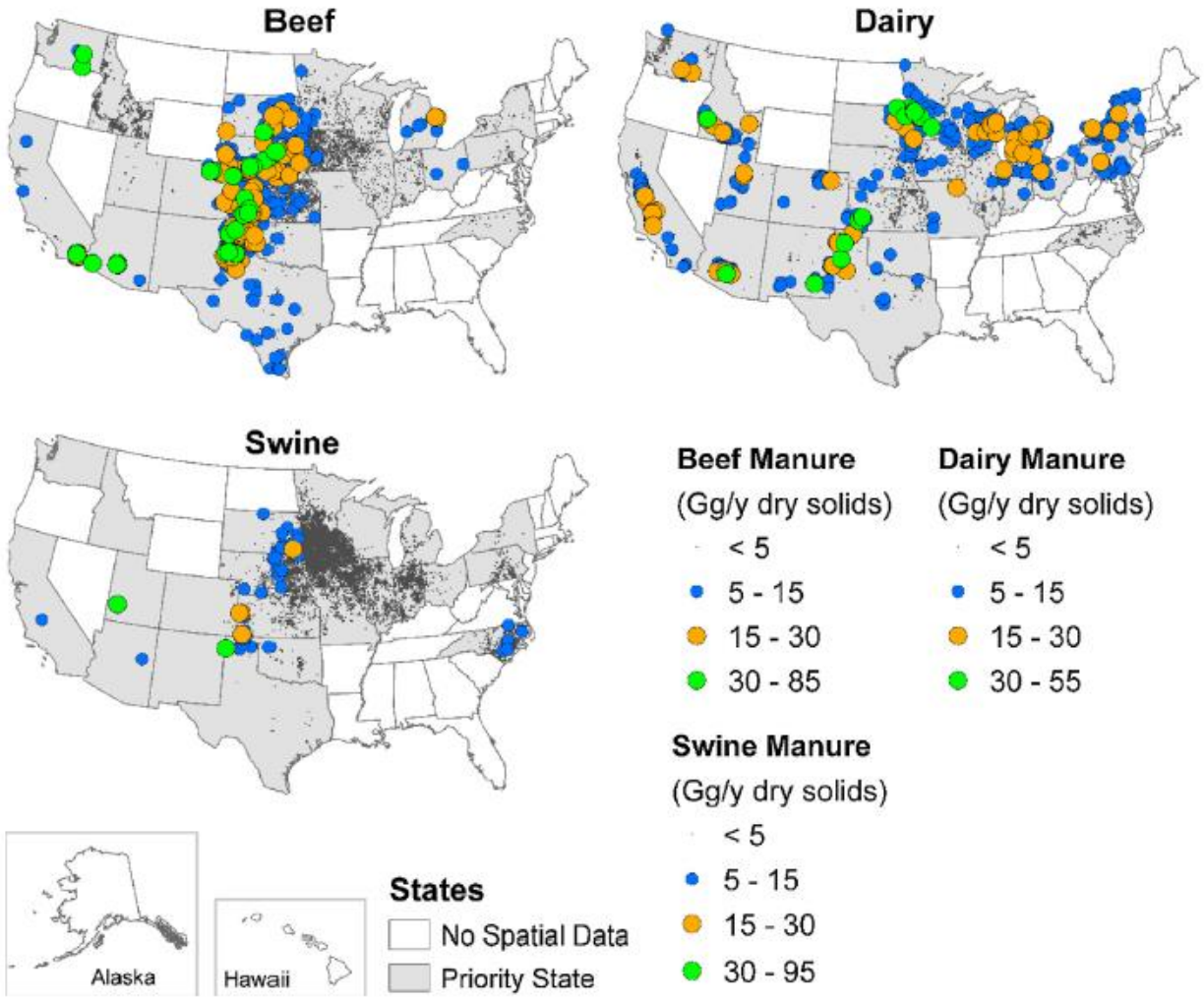

Source: Milbrandt 2018

Appendix Figure A.4. Water-level changes in the Ogallala Aquifer from 1950s to 2015

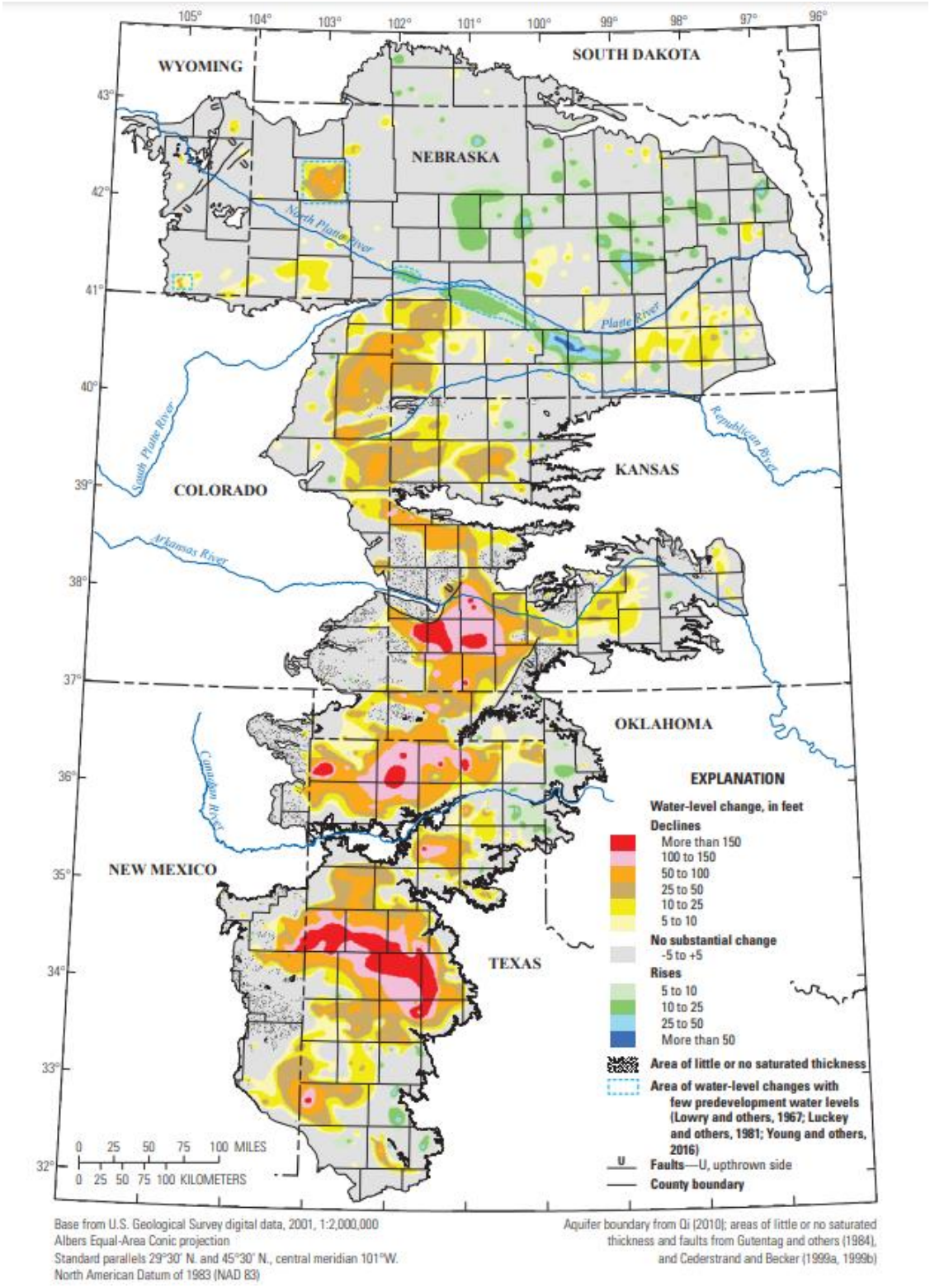

Source: USGS 2001

Appendix Figure A.5. Lab-scale gas-sparged AnMBR at Kansas State University

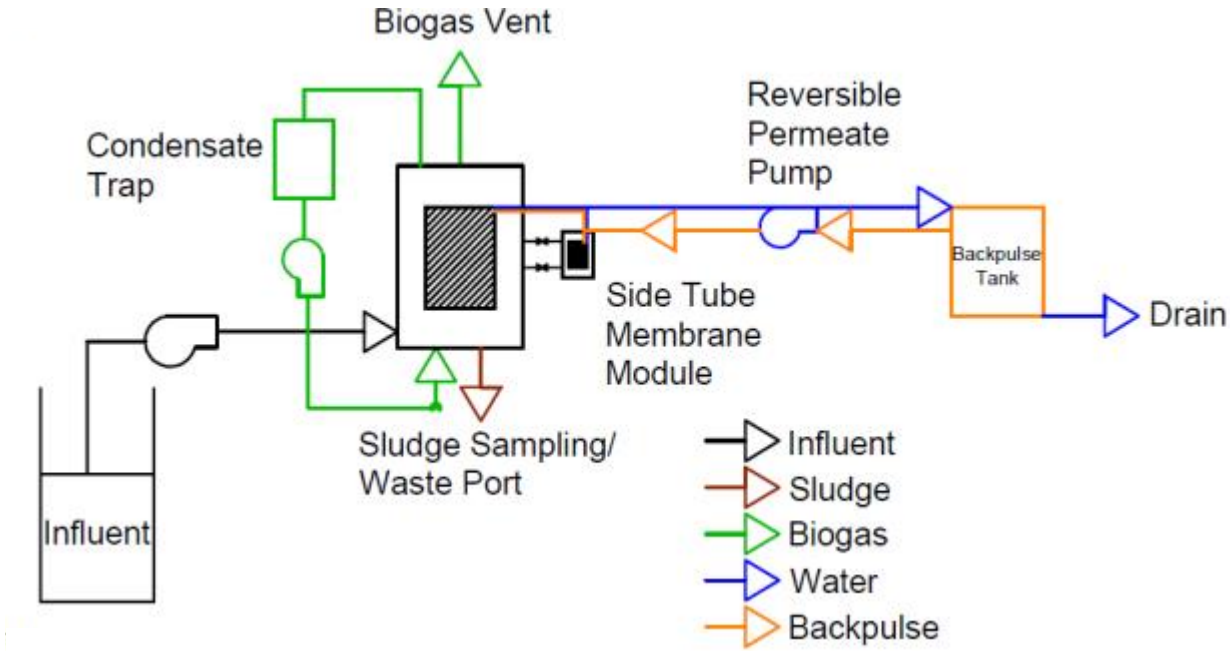

Source: Lim's dissertation

Appendix Figure A.6. Calculated actual NH3(mg/L) in varying solutions with respect to time. pH 8, 9, 10, 12 solutions include quantities of NaOH

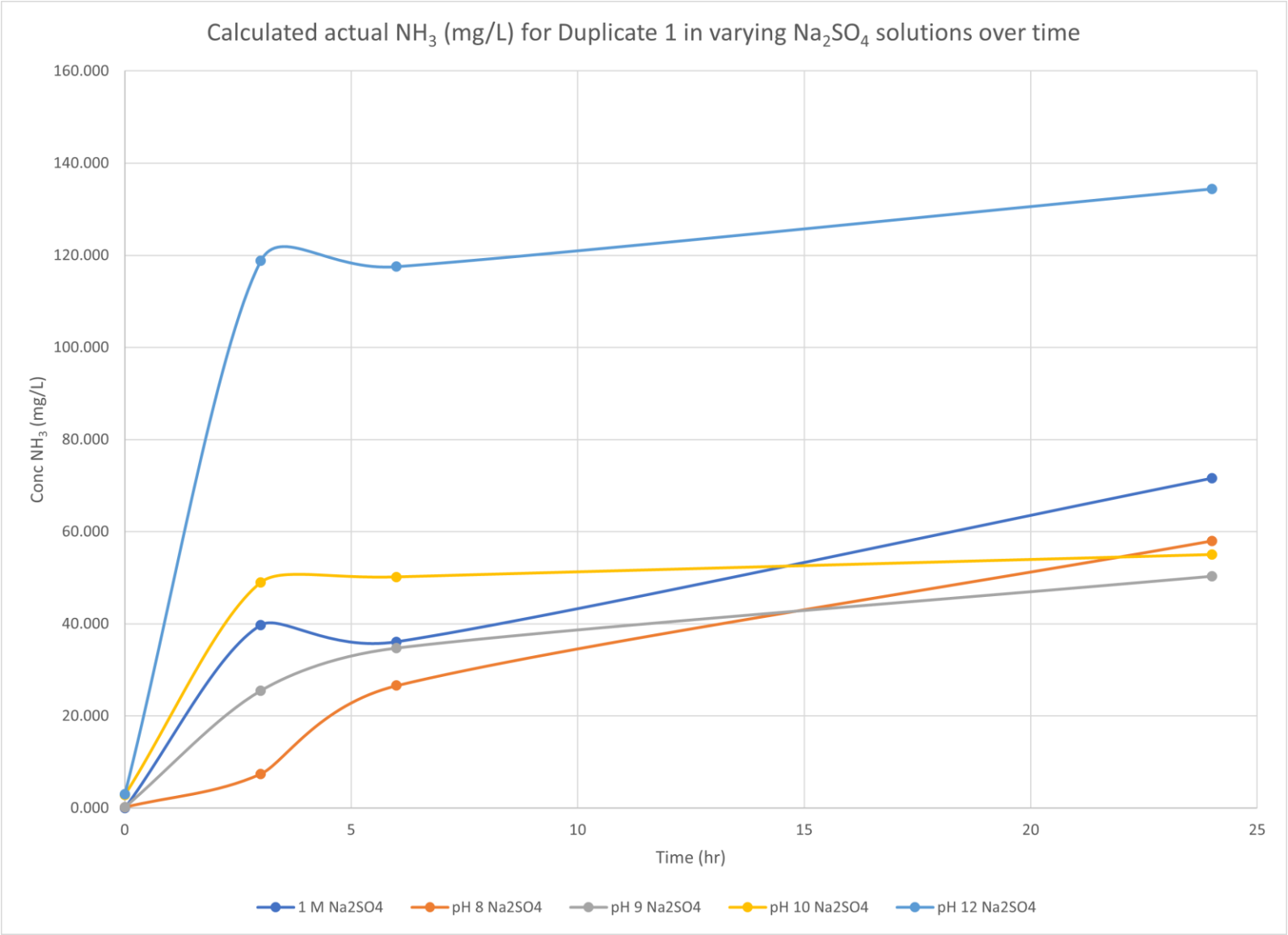

Appendix Figure A.7. Calculated actual NH4+ (mg/L) in varying solutions with respect to time. pH 8, 9, 10, 12 solutions include quantities of NaOH

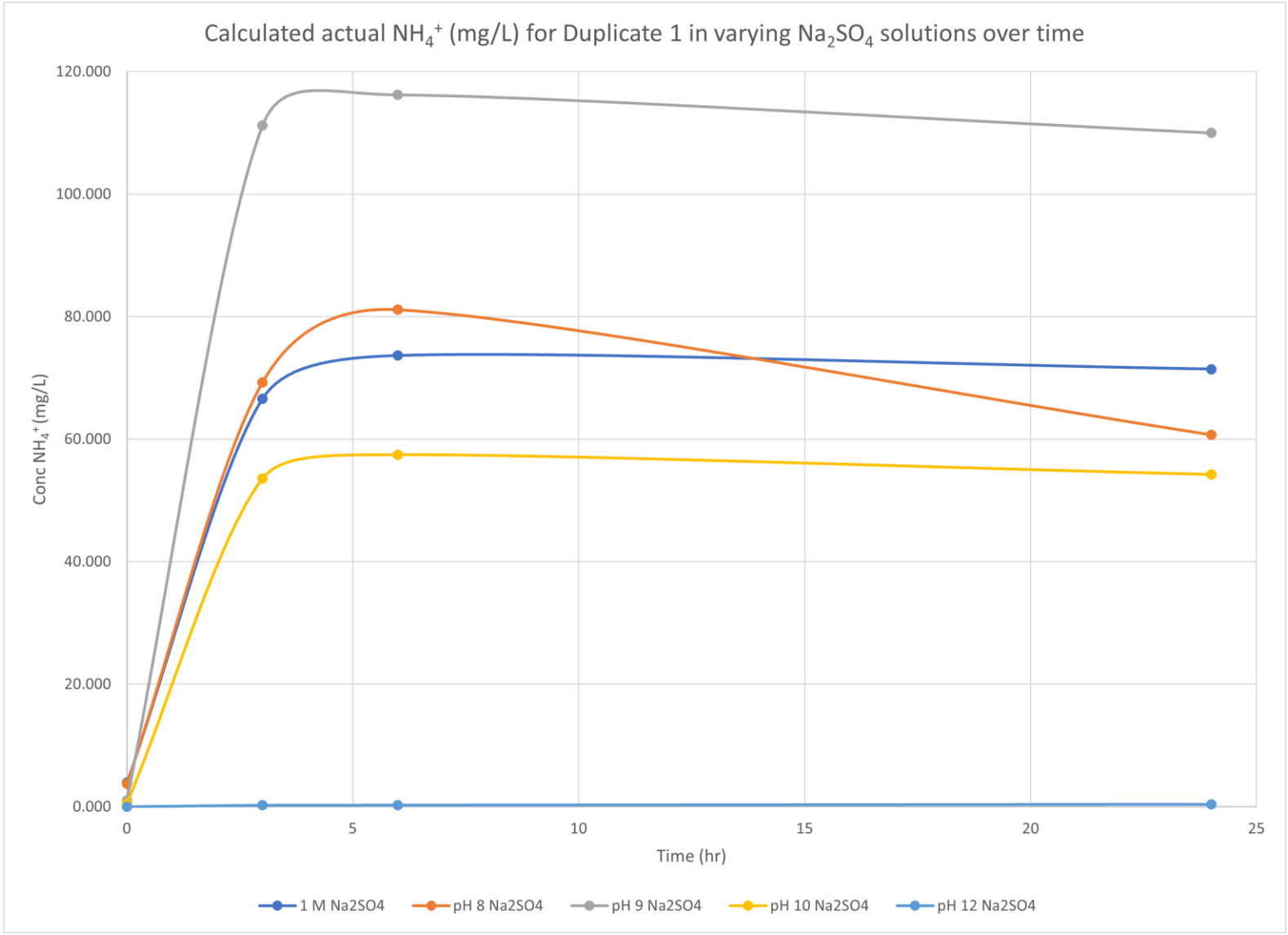

Appendix Figure A.8. Calculated actual NH3(mg/L) in varying solutions with respect to time. pH 8, 9, 10, 12 solutions include quantities of NaOH

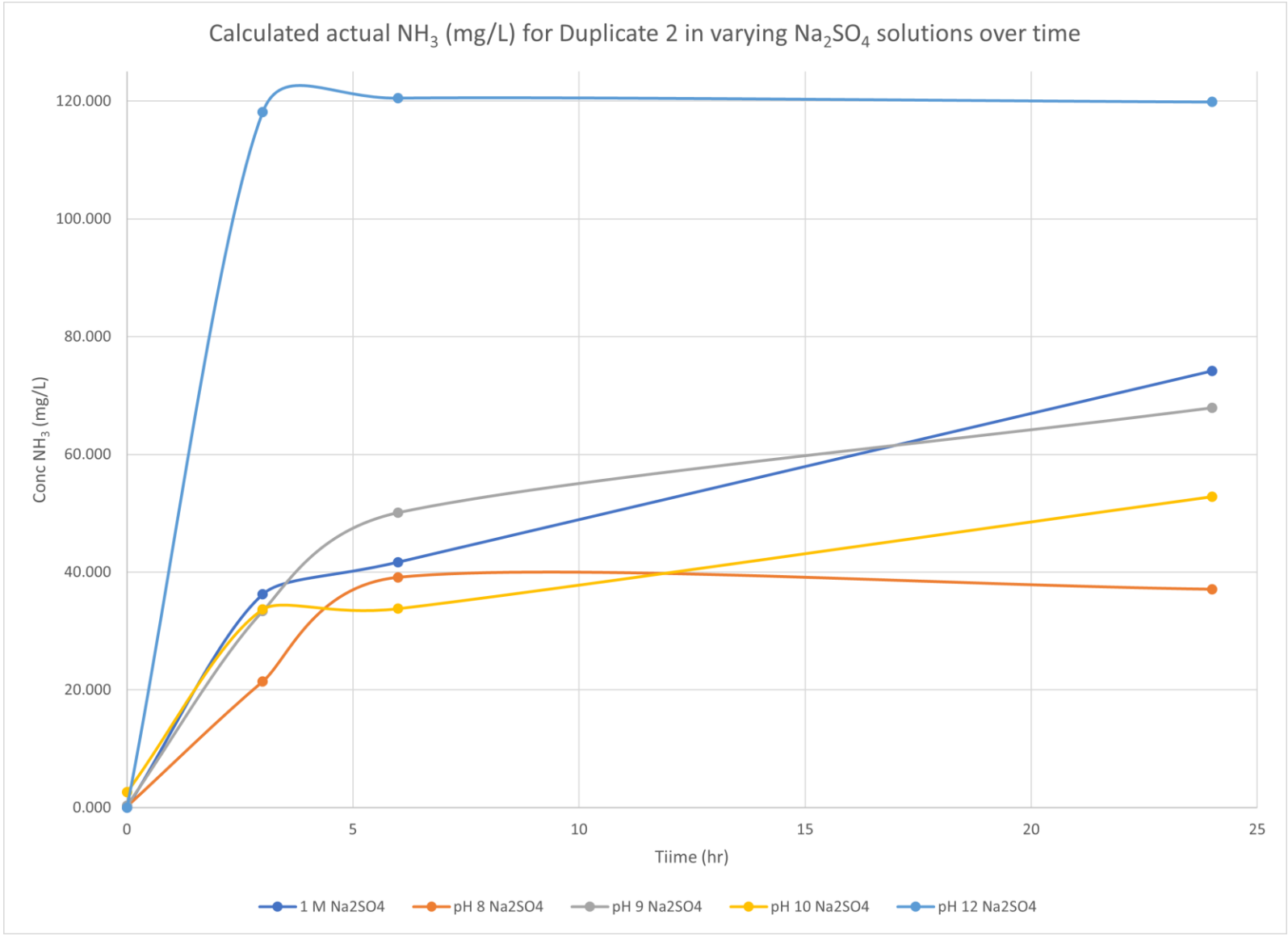

Appendix Figure A.9. Calculated actual NH4+(mg/L) in varying solutions with respect to time. pH 8, 9, 10, 12 solutions include quantities of NaOH

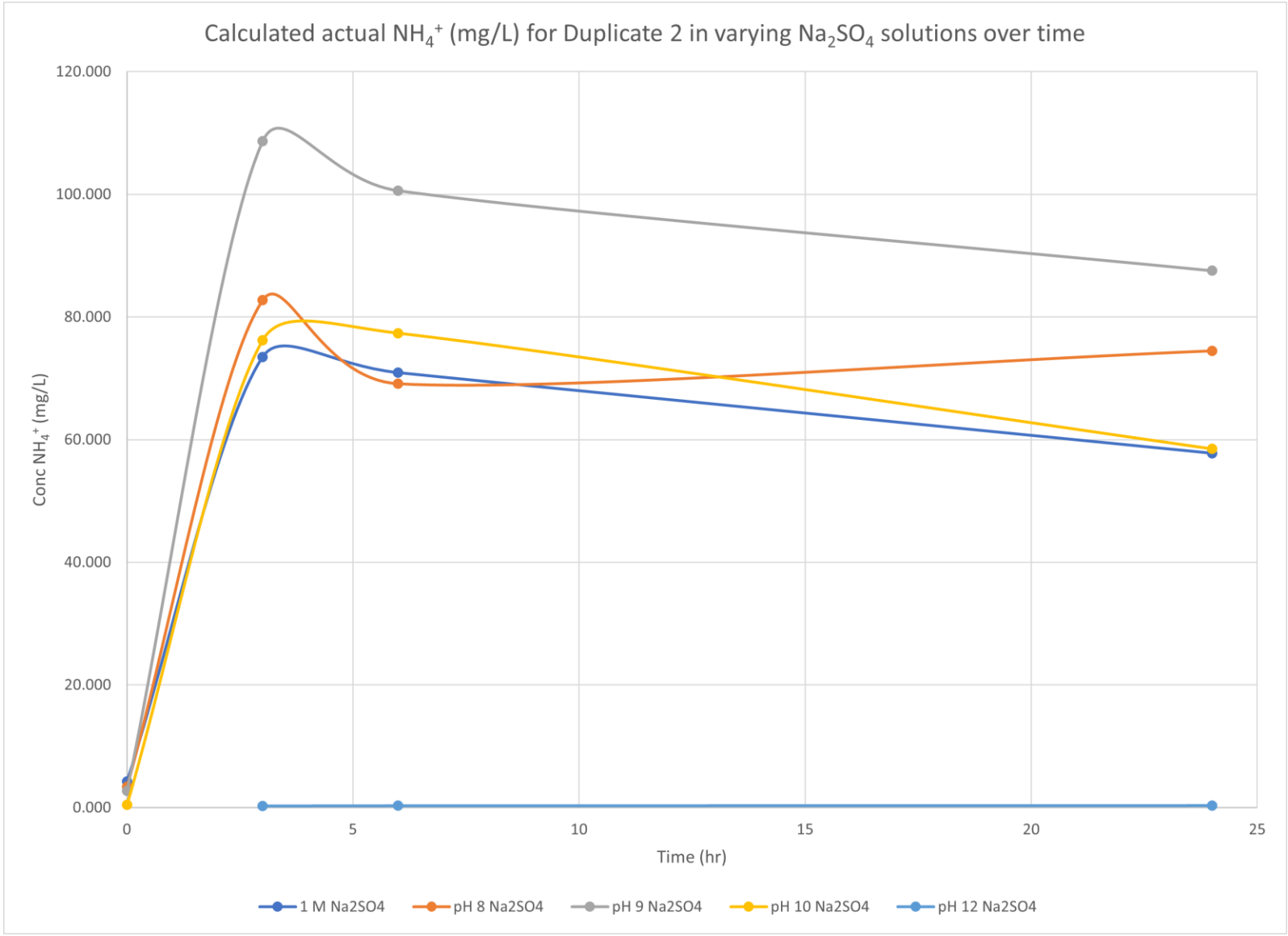

Appendix Figure A.10. Calculated percentages of ammonia and ammonium in solution for duplicate 1. pH 8, 9, 10, 12 solutions include quantities of NaOH.

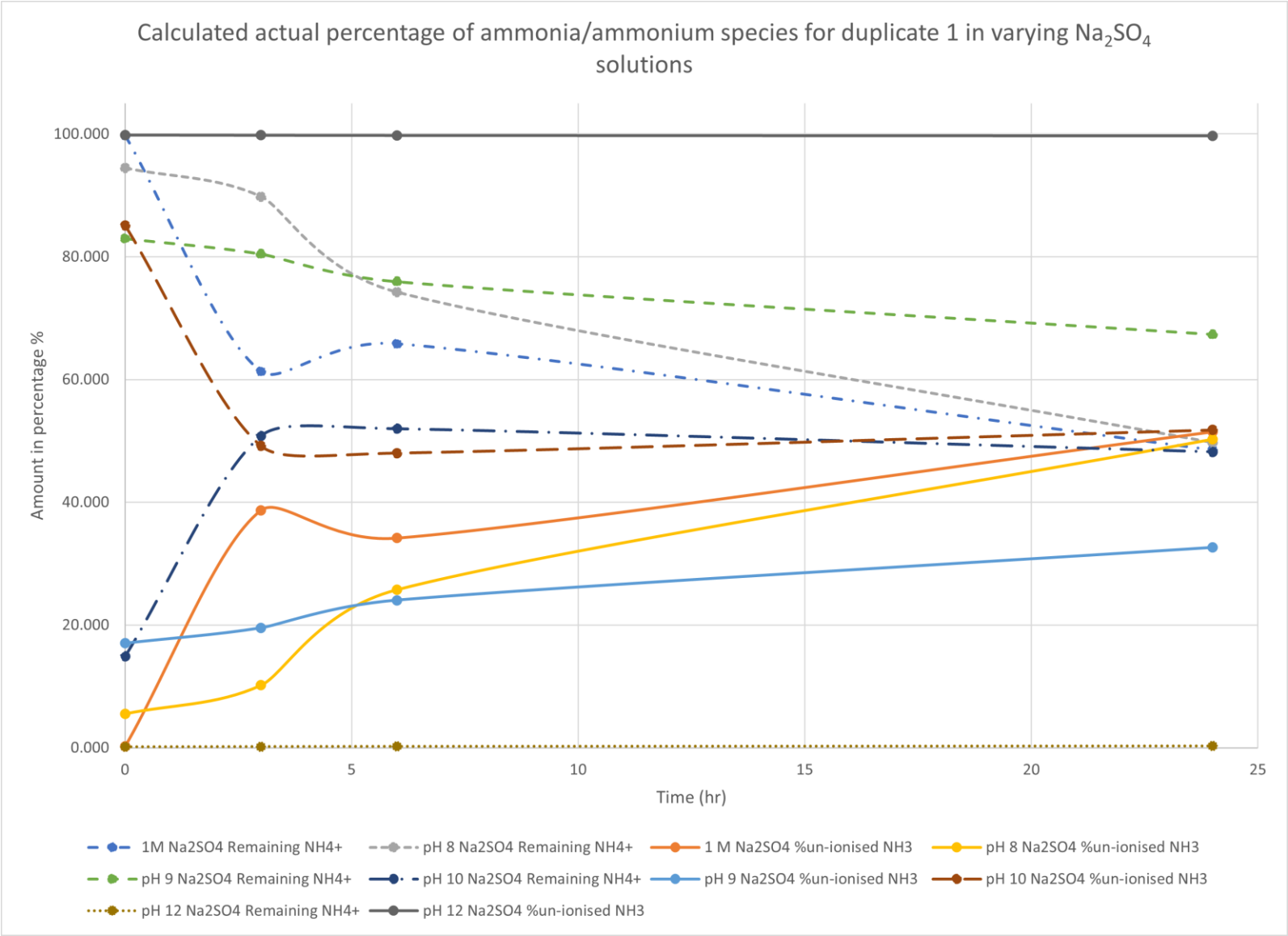

Appendix Figure A.11. Calculated percentages of ammonia and ammonium in solution for sample 2. pH 8, 9, 10, 12 solutions include quantities of NaOH.

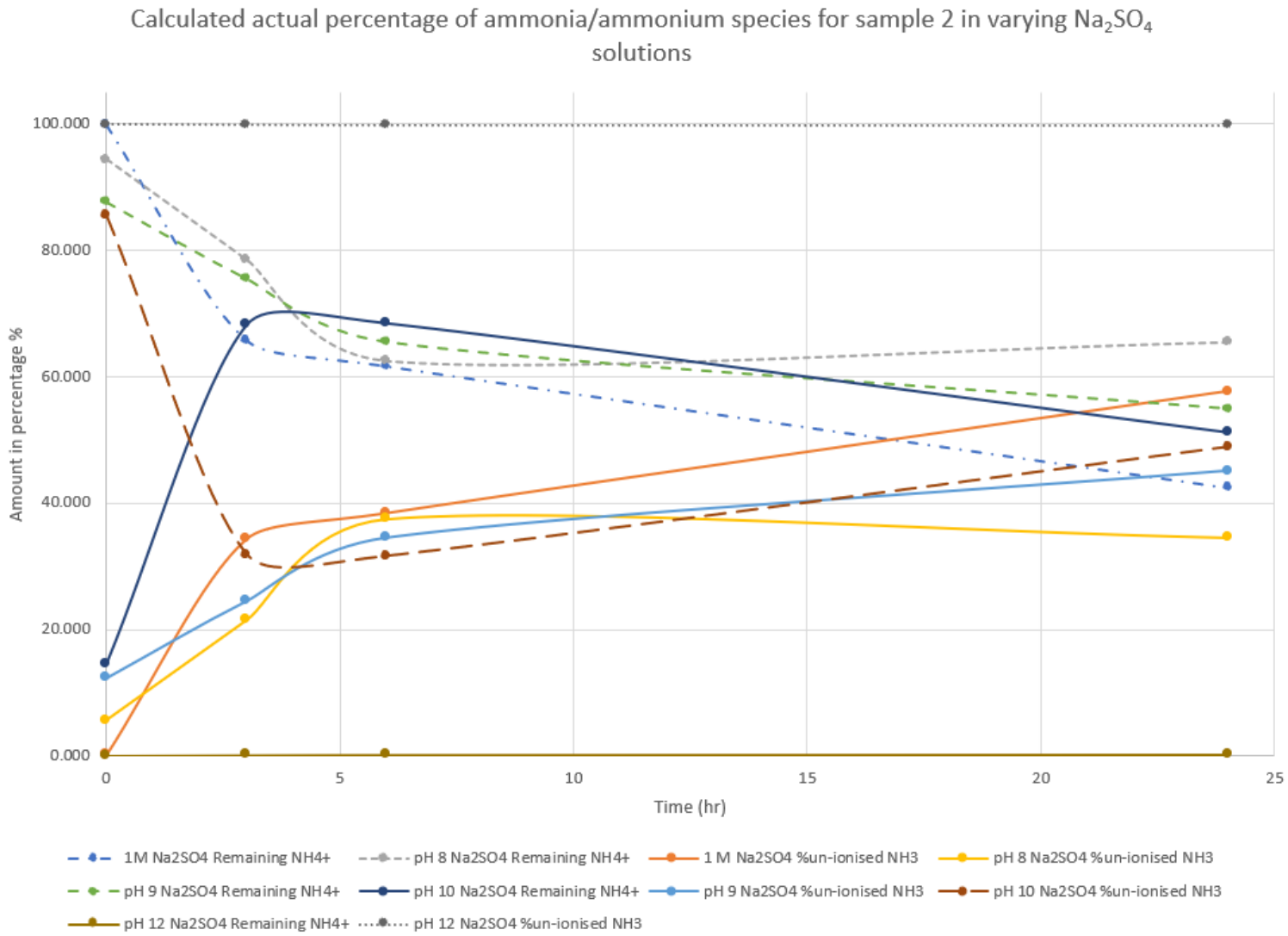

Appendix Figure A.12. Ratio between ammonia and ammonium species with respect to pH. Credit: Image used for educational purposes, Seneye